CHAPTER - III

SCATTERING OF ELECTRONS BY HYDROGEN ATOMS

3.1. Introduction :

Electron scattering from atomic hydrogen (H), (z = 1) is one of the most basic problems in atomic Physics. In this case all the states of the target (hydrogen) are known exactly so there can be no uncertainty in the amplitude arising from the use of bound state wave functions. On the other hand experiments in atomic hydrogen must be performed in a crossed - beam configuration. Because the tendency of atomic hydrogen to form molecule of H_2 , it was difficult to do precise experiments. This difficulty was resolved in the recent years. We have now the experimental results for DCS .

In the present study, first we consider all types of collision processes for the interaction of electron with the hydrogen atom, at the incident energies 100 to 700 eV. Two basic approximations (Yates 1974, 1979) are used in these studies. The exchange effects are included in the DCS calculations. Ochkur (1963) approximation is used to calculate the exchange scattering amplitudes. The DCS's

are calculated through $O(k_i^{-2})$ in the present investigations. The scattering amplitude for DCS is given as

$$F_{HHOB} = f^{(1)}_{i\to f} + \mathrm{Re1}\, f^{(2)}_{HEA} + \mathrm{Re2}\, f^{(2)}_{HEA} + \mathrm{Im}\, f^{(2)}_{HEA} + g_{och} + f^{(3)}_{GES} \qquad (3.1)$$

The DCS $O(k_i^{-2})$ is approximated from (3.1) for fixed q.

$$\frac{d\sigma}{d\Omega} = \frac{k_f}{k_i} \left| F_{HHOB} \right|^2 \qquad (3.2)$$

In the above equation (3.1) first term is the usual first Born amplitude (2.12) second, third and fourth terms are the real and imaginary parts of the second Born approximation (equation 2.57), fifth and sixth terms are the exchange (Ochkur, 1963) (equation 2.36) and third GES term (Yates, 1974) (equation 2.45). The following problems for $\bar{e}$ - H atom collision processes are studied in the present chapter.

i) Elastic scattering of electrons by the ground state of hydrogen atom (1s - 1s)

ii) Elastic scattering of electrons by the excited state of hydrogen atom (2s - 2s)

iii) Inelastic scattering of electrons by hydrogen atom (1s - 2s)

iv) Born exchange amplitudes in HEA .

The total collisional cross sections are calculated using the optical theorem (Taylor, 1972). The TCS's are obtained from the following expression.

$$\sigma = \frac{4\pi}{k_i} \; \mathrm{Im} \; f^{(2)}_{HEA} (0) \qquad (3.3)$$

The TES's are calculated through equations (1.7) and (3.2).

3.2.1 Elastic scattering of electrons by the ground (1s) state of hydrogen atom (ESGH).

$$\bar{e} + H (1s) \longrightarrow \bar{e} + H (1s) \qquad (3.4)$$

In the elastic process equation (1.1) the final state function of the target hydrogen atom is same as the initial ground state function. The ground state wave function for the hydrogen atom can be written as

$$\Psi_{1s} (r_1) = \frac{1}{\pi^{1/2}} \exp (- r_1) = A \exp (- r_1) \qquad (3.5)$$

The product of the wave functions for initial 1s and final 1s states can be written as

$$\psi_i(r_1)\,\psi_f^*(r_1) = A^2 \exp(-2r_1)$$

$$= -A^2 D^n(y)\,\frac{\exp(-yr_1)}{r_1}$$

$$= -A^2 \frac{\partial^n}{\partial^n y}\,\frac{\exp(-yr_1)}{r_1}\Bigg|_{\substack{n=1,\\ y=2}} \qquad (3.6)$$

For the convenience for the study of the scattering processes, the product of the wave functions was written in the derivative form. $D^n(y)$ stands for the differentiation w.r.t y and n stands for the order of the corresponding differentiation. At the end of calculations the values for A^2 ($= \pi^{-1}$), y ($= 2$) and $n=1$ are substituted.

The interaction equation (2.24) between $\bar{e}$ - H atom can be written as

$$V_d = -\frac{1}{r_o} + \frac{1}{|\underline{r}_o - \underline{r}_1|} \qquad (3.7)$$

where $\underline{r}_o$ and $\underline{r}_1$ are the position vectors of the incident electron and target hydrogen w.r.t the target nuclei. Substituting equations (3.6, 3.7) in the equations (2.12, 2.57, 2.36, 2.43) we will obtain the corresponding scattering amplitudes for the DCS equation (3.2). All these contributions to the DCS can be obtained as follows.

$$f^{(1)}_{i\to f} = -\frac{1}{2\pi}\int d\,\underline{r}_o \exp(i\,\underline{q}.\underline{r}_o)\,V_{fi}(\underline{r}_o)$$

$$= -\frac{1}{2\pi}\iint d\,\underline{r}_o\, d\,\underline{r}_1 \exp(i\,\underline{q}.\underline{r}_o)\,V_d$$

$$\psi^*_f(r_1)\,\psi_i(r_1)$$

$$= A^2\, 2\pi\, \frac{(q^2 + 2y^2)}{(q^2 + y^2)^2}$$

$$= 2\,\frac{(q^2 + 8)}{(q^2 + 4)^2} \qquad (3.8)$$

This expression is the first Born approximation for hydrogen atom. Now the imaginary and real parts of the second Born approximation are obtained as

$$\mathrm{Im}\, f^{(2)}_{HEA} = \frac{4\pi^3}{k_i}\int d\underline{p}\; U^{(2)}_{fi}(\underline{q} - \underline{p} - \beta_i\hat{y}\,;\,\underline{p} + \beta_i\hat{y})$$

$$= \frac{4\pi^3}{k_i}\int d\underline{p} \langle \psi^*_f(r_1)|\,\bar{V}(\underline{q} - \underline{p} - \beta_i\hat{y}\,;\,r_1)$$

$$\bar{V}(\underline{p} + \beta_i\hat{y}\,;\,r_1)|\,\psi_i(r_1)\rangle \qquad (3.9)$$

Using the equation (2.53) for $\bar{V}$ (------)'s in the above matrix element, it reduces to

$$= \frac{1}{\pi k_i} \int d\underline{p} \int d\underline{r}_1 \, [\exp(i(\underline{q} - \underline{p}).\underline{b}_1 - i\beta_i Z_1) - 1]$$

$$[\exp(i\,\underline{p}.\underline{b}_1 + i\beta_i Z_1) - 1]$$

$$\psi_i(r_1)\,\psi_f^*(r_1)/(|\underline{q} - \underline{p}|^2 + \beta_i^2)(p^2 + \beta_i^2)$$

$$= -\frac{A^2}{\pi k_i} D(y) \int \frac{d\underline{p}}{(|\underline{q} - \underline{p}|^2 + \beta_i^2)(p^2 + \beta_i^2)}$$

$$\int \frac{d\underline{r}_1}{r_1} \exp(-yr_1)$$

$$[\exp(i(\underline{q} - \underline{p}).\underline{b}_1 - i\beta_i Z_1) - 1]$$

$$[\exp(i\,\underline{p}.\underline{b}_1 + i\beta_i Z_1) - 1] \qquad (3.10)$$

The typical solution of the $d\underline{r}_1$ integral is

$$\int \frac{d\underline{r}_1}{r_1} \exp(-yr_1) \exp(i\,\underline{Q}.\underline{r}_1) = \frac{4\pi}{(Q^2 + y^2)}$$

Using this the above $d\underline{r}_1$ integral can be evaluated very easily.

$$= -\frac{4A^2 D(y)}{k_i} \int \frac{d\underline{p}}{(|\underline{q} - \underline{p}|^2 + \beta_i^2)(p^2 + \beta_i^2)}$$

$$[\ \frac{(q^2 + 2y^2)}{y^2(q^2 + y^2)} - (\ |\underline{g} - \underline{p}\ |^2 + \beta_i^2 + y^2\ )^{-1}$$

$$- (\ p^2 + \beta_i^2 + y^2\ )^{-1}\ ]$$

$$= - \frac{4\ A^2\ D(\ y\ )}{k_i} \int \frac{d\underline{p}}{(\ |\underline{g} - \underline{p}\ |^2 + \beta_i^2\ )(\ p^2 + \beta_i^2\ )}$$

$$[\ \frac{(\ q^2 + 2y^2\ )}{y^2(\ q^2 + y^2)} - 2$$

$$(\ p^2 + \beta_i^2 + y^2\ )^{-1}\ ]$$

$$= - \frac{4\ A^2\ D(\ y\ )}{k_i} \int \frac{d\underline{p}}{(\ |\underline{g} - \underline{p}\ |^2 + \beta_i^2\ )\ y^2}$$

$$[\ \frac{2}{(\ p^2 + \beta_i^2 + y^2\ )} - \frac{q^2}{(q^2 + y^2)(p^2 + \beta_i^2\ )}\ ]$$

This integrand is obtained by using the partial fraction technique. Few integrand terms are cancelled with the opposite same type of terms after partial fraction. After the evaluation of the two dimensional $d\underline{p}$ integral (given in the appendix) the closed form of the imaginary contribution can be given as

$$\mathrm{Im}\ f^{(2)}_{HEA} = -\frac{4A^2}{k_i} D(y) \frac{1}{y^2} [\, 2 I_1(\beta_i^2, y^2)$$

$$- \frac{q^2}{(q^2 + y^2)} I_1'(\beta_i^2, 0)\,] \qquad (3.11)$$

where $I_1(\beta_i^2, y^2)$ is a function of β_i^2, q^2 and y^2, and $I_1'(\beta_i^2, 0)$ is a function of only β_i^2 and q^2. These are given as

$$I_1(\beta_i^2, y^2) = \frac{\pi}{E} \log$$

$$\left[\frac{(q^2 + \beta_i^2)(E + q^2 + y^2) + 2\beta_i^2 (q^2 - y^2)}{(\beta_i^2 + y^2)(E - q^2 - y^2)} \right]$$

$$E^2 = (q^2 + y^2)^2 + 4q^2\beta_i^2$$

and

$$I_1'(\beta_i^2, 0) = I_1(\beta_i^2, y^2) \Big|_{y=0}$$

In the forward direction ($q = 0$) the TCS expression is obtained from equations (3.3) and (3.11).

$$\sigma^H_{tot} = -\frac{32\pi}{k_i^2} D(y) \frac{1}{y^4} \log \left[\frac{(\beta_i^2 + y^2)}{\beta_i^2} \right] \qquad (3.12)$$

The TCS results are shown in the table (3.4).

The $d\underline{r}_1$ evaluation of the real part of order k_i^{-1} (equation 2.58) is exactly same as imaginary part. Using the above results of imaginary part, the real part $O(k_i^{-1})$ is given as

$$\mathrm{Rel}\ f^{(2)}_{HEA} = \frac{4A^2}{\pi k_i} D(y) \mathcal{P} \int d\underline{p} \int_{-\infty}^{\infty} \frac{dp_Z}{(p_Z - \beta_i)} \frac{1}{y^2} \frac{1}{(|\underline{q} - \underline{p}|^2 + p_Z^2)} \left[\frac{2}{(p^2 + p_Z^2 + y^2)} - \frac{q^2}{(p^2 + p_Z^2)(q^2 + y^2)} \right]$$

After, performing the $d\underline{p}$ and dp_Z integrals (given in appendix), the closed form of this scattering amplitude can be obtained as

$$\mathrm{Rel}\ f^{(2)}_{HEA} = \frac{4A^2}{\pi k_i} D(y) \frac{1}{y^2} \left[2 I_2(\beta_i^2, y^2) - \frac{q^2}{(q^2 + y^2)} I_2'(\beta_i^2, 0) \right] \qquad (3.13)$$

where

$$I_2\,(\beta_i^2\,,\,y^2) = -\frac{\pi^3}{E}\left[\,1 - \mathrm{Sgn}(y^2 - q^2)\left(\frac{1}{2} - \frac{\sin^{-1}Y}{\pi}\right)\right]$$

$$Y = 1 - \frac{2\beta_i^2\,(\,y^2 - q^2)^2}{(y^2 + q^2)^2(\beta_i^2 + y^2\,)}$$

$$\mathrm{Sgn}(y^2 - q^2) = \frac{(y^2 - q^2)}{|y^2 - q^2|} = \begin{matrix} +1 & y > q \\ -1 & y < q \end{matrix}$$

$$I_2'\,(\beta_i^2\,,\,0) = I_2\,(\beta_i^2\,,\,y^2)\,\Big|_{y=0}$$

Now the integrals in the real part of the second Born term of $O\,(\,k_i^{-2}\,)$ equation (2.59) are same as real part of $O\,(\,k_i^{-1}\,)$. Here the integrand is simpler than the real part of $O\,(\,k_i^{-1}\,)$ because of the cancellation of $(\,p^2 + p_Z^2\,)$ term with the same type of denominator term. This corresponding form of the real part after the $d\underline{r}_1$ integration is given as

$$\mathrm{Re}2\;f^{(2)}_{HEA} = \frac{2\,A^2}{\pi k_i^2}\,D\,(\,y\,)\,D'\mathcal{P}\int d\underline{p}\int_{-\infty}^{\infty}\frac{dp_Z}{(p_Z - \beta_i)}$$

$$\frac{1}{(\,|\underline{q} - \underline{p}\,|^2 + p_Z^2\,)}\left[\,\frac{(\,q^2 + 2y^2)}{y^2(\,q^2 + y^2)} - (|\underline{q} - \underline{p}\,|^2 + p_Z^2 + y^2\,)^{-1} - (p^2 + p_Z^2 + y^2)^{-1}\,\right]$$

.....(3.14)

Following the same procedure for $d\underline{p}$ and $d\underline{p}_Z$ integrals as discussed above, the closed form of this real part can be obtained as

$$\mathrm{Re}2 \; f^{(2)}_{HEA} = \frac{2\,A^2}{\pi k_i^2} \, D(y) \, D' \left[\frac{I_3'(\beta_i, 0)}{q^2 + y^2} + \frac{I_3(\beta_i, y)}{y^2} - I_2(\beta_i^2, y^2) \right] \qquad (3.15)$$

where

$$I_3(\beta_i, y) = -\pi^3 \left(1 - \frac{2}{\pi} \tan^{-1} \frac{y}{\beta_i} \right)$$

$$I_3'(\beta_i, 0) = I_3(\beta_i, y) \big|_{y=0}$$

D' is differential operator w.r.t β_i .

The third GES term equation (2.45) given by Yates (1974) is reformulated in a convenient form for the purpose of the present study. This term was given with a differential operator acting on a dimensionless vector T ($= q/y$). In the present study we have introduced the $D(y)$ operator using the partial differentiation technique, instead of the T differentiation. The modified form the equation (2.45) is obtained as

$$f^{(3)}_{GES} = -\frac{y^4 \pi A^2}{16 k_i^2} \, D(y) \, (q^2 + y^2)^{-1} \left[4 \left\{ \log \left(\frac{q^2 + y^2}{yq} \right) \right\}^2 + \right.$$

$$\frac{\pi^2}{3} - 2A(q, y^2)\,]\,|_{y=2}$$

$$= -\frac{y^4\,\pi}{16\,k_i^2}\,A^2\,D(y)\,F(q, y) \qquad (3.16)$$

where

$$A(q, y^2) = 2\left(\log\frac{q}{y}\right)^2 + \frac{\pi^2}{6} + \sum_{n=1}^{\infty}\frac{(-q^2/y^2)^n}{n^2}, \quad \frac{q}{y} \leq 1$$

$$= -\sum_{n=1}^{\infty}\frac{(-y^2/q^2)^n}{n^2}, \qquad \frac{q}{y} > 1$$

Finally for the consistent picture of DCS $O(k_i^{-2})$ we have included the first term of the exchange amplitude equation (2.36) using the Ochkur approximation (Joachain , 1975). This exchange contribution is obtained as

$$g_{och} = -\frac{2}{k_i^2}\int d\underline{r}_1\,\exp(i\underline{q}\cdot\underline{r}_1)\,\psi_i(r_1)\,\psi_f^*(\underline{r}_1)$$

$$= \frac{8\,\pi\,A^2}{k_i^2}\,D(y)\,(q^2 + y^2)^{-1}$$

$$= -\frac{32}{k_i^2}(q^2 + 4)^{-2} \qquad (3.17)$$

3.2.2 <u>Comparison of present ESGH results with the other data</u> :

Using the scattering amplitudes (equations 3.8, 3.11,

3.13, 3.15, 3.16, 3.17) derived under the assumptions of HEA (Sec. 2.3.5) and GES (Sec. 2.3.4), I have performed detailed calculations (DCS , TCS) for the ESGH process (Sec. 3.2.1) in the energy range 100 - 700 eV. I used an average excitation energy DE = 0.465 a.u (Byron and Joachain, 1977) in the calculation of second Born term (equations 3.11, 3.13, 3.15). Our HHOB DCS and TCS are presented in the Tables (3.1, 3.2) and (3.4) as well as in the form of graphs shown in Figs. (3.1, 3.2) along with the other theoretical and experimental data. As it was expected the present results are found to be in good agreement with the compared data in the angular range $\theta \leq 50$. The details of our comparisons with the present DCS and TCS are as follows.

Fig. (3.1) shows the present DCS (Solid curves a,b) along with the recent theoretical and experimental data at incident energy E = 100 eV. The solid curves a and b are obtained by using the results given in Table (3.1) with and without real part O ($\bar{k}_i^{-2}$) in the DCS (equation 3.2) calculation. These two curves are compared with the recent experimental data, O - Van Wingerden et al , (1977) and theoretical results, + — EBS (eikonal Born series) of Byron and Joachain (1981), ⊙ — UEBS (Unitarised eikonal Born series) of Byron et al , (1982)

and ● — EOM (Elicit Optical Model) of Mc Carthy et al , (1981). It can be observed from the figure that curve a approaches the compared theoretical results in the absence of real part O (k_i^{-2}) (i.e. curve b). But curve b is away from the compared experimental data, which shows the importance of real part O (k_i^{-2}) in the small angle region. The present DCS curve a is found to be in good agreement with the compared data at scattering angles $\theta \leq 30^o$, and satisfactory in the angular range between 30 and 60°.

Fig. (3.2) shows the present DCS (Solid curve a' without exchange (equation 3.17) in (equation 3.1)) at incident energies 100 (set A), 200 (set B) and 400 (set C) eV in the angular range $\theta \leq 60^o$. This figure represents three sets of results. In set A, the present DCS are compared with the recent theoretical results , ▲ — C C S O P M (Coupled - Channel Second Order Potential Model) of Bransden et al , (1982), and the experimental results, O — Van Wingerden et al , (1977) (renormalised results of Lloyd et al, 1974) and ● — Williams (1975) at incident energy E = 100 eV . Similar type comparisons are shown in set B and set C at incident energies E = 200 and 400 eV respectively. With respect to the experimental data the present results are better than the

compared theoretical results . Again in the absence of exchange (equation 3.17) and real part (equation 3.14) contributions to the DCS (equation 3.2) the present results fall considerably under the compared experimental and theoretical results (not shown in the Fig. 3.2). This can be noted from a careful comparison of Fig.(3.1) and Fig. (3.2) at 100 eV.

Figs. (3.1) and (3.2) show the important of exchange and real part O (k_i^{-2}) to obtain agreement with the recent experimental data. Even with the Ochkur,(1963) exchange first order correction, the present DCS results (curve a) are found slightly lower than the recent experimental results. These present DCS results can be improved by the inclusion of higher order exchange correction , (Solid curve C in Fig. 3.2 shows these results which will be discussed later) to the direct scattering amplitude (equation 3.1) of HHOB .

Our HHOB results for ESGH process are listed in Tables (3.2 and 3.4) in the energy range 100 to 700 eV. Table (3.1) shows all the scattering amplitudes i.e. first Born (equation 3.8) real parts of second Born (equations 3.13 , 3.15) and third GES (equation 3.16) and First order exchange (equation 3.17), and the imaginary part of the second Born (equation 3.11), in the angular range

$\theta \leq 120^{o}$, and at incident energies 100, 200, and 400 eV. The DCS (equation 3.2) calculated using all these scattering amplitudes without and with Ochkur exchange term (equation 3.17) are also listed. Table (3.2) shows only DCS without exchange correction in the angular region $\theta \leq 60^{o}$, and at incident energies 100 to 700 eV. Table (3.4) shows the present TCS (equation 3.12) at the incident energies 100 to 700 eV., along with the compared theoretical and experimental data. The present DCS and TCS are found to be in good agreement with the compared results. And this agreement was better at higher incident energies than at 100 eV.

From Table (3.1) it can be observed that the real part (equation 3.15), O (k_i^{-2}) behaves entirely different than the remaining terms. This term is fluctuating in the entire scattering angular region. This is due to the presence of oscillating terms in equation (3.15). In real part (equation 3.13), O (k_i^{-1}) also slight fluctuations are observed, but these are comparatively negligible than in equation (3.15). More or less equation (3.15) is behaving like third GES term equation (3.16). These points will be discussed in the last chapter.

So far we considered the ESGH process. The DCS and TCS results for this process are very encouraging for the

further study of the collisional processes. This gave us a scope to study the scattering of electrons from the metastable 2s state of hydrogen atom (Rao and Desai, 1983a). This type of elastic process plays an important role in the plasma and astrophysics. In the recent past, very few approximations were applied for this process (Joachain et al, 1977a,b ; Joachain and Winters, 1980 ; Pundir et al, 1982). In this work we made an attempt for the study of this process, which is described in the following section.

3.3.1 Elastic scattering of electrons by the excited (2s) state of hydrogen atom (ESEH) : (Rao and Desai, 1983a).

$$\bar{e} + H^{*}(2s) \longrightarrow \bar{e} + H^{*}(2s) \qquad (3.18)$$

The approximation methods applied for ESGH study discussed in the above sections can be applied to this scattering process (equation 1.3), in which the target hydrogen atom is initially in an excited 2s state (equation 3.18). The scattering amplitudes in ESGH (equations 3.8, 3.11, 3.13, 3.15, 3.16 , 3.17) can be extended to this present ESEH study . Here it is assumed that the target electron is initially in the 2s excited state of hydrogen atom. The wave function corresponding to this state is

$$\psi_{2s}(r_1) = \frac{1}{4(2\pi)^{1/2}} (2 - r_1) \exp(-r_1/2)$$

$$= (B + A\, r_1)\, \exp(-r_1/2) \qquad (3.19)$$

where

$$B = 0.19947, \quad A = -0.099736.$$

The final state of hydrogen atom is assumed as initial 2s state. The product of the initial and final wave functions can be obtained as

$$\Psi_i(r_1)\, \Psi_f^*(r_1) = \Psi_{2s}(r_1)\, \Psi_{2s}^*(r_1)$$

$$= (B + A\, r_1)^2 \exp(-r_1)$$

$$= (B^2 + 2ABr_1 + A^2 r_1^2) \exp(-r_1) \qquad .....(3.20)$$

where B^2, $2AB$ and A^2 are constants that can be obtained from the normalisation coefficients of the 2s wave function of target hydrogen (equation 3.19). The product of the wave functions (equation 3.20) can be written with the differential operator $D^n(y)$(equation 3.6).

$$= [-B^2 D^1(y) \exp(-y\, r_1) + 2\, A\, B\, D^2(y) \exp(-y\, r_1) - A^2 D^3(y) \exp(-y\, r_1)] \frac{1}{r_1}$$

$$= -\sum_{n=1}^{3} [B_n' D^n(y) \exp(-y\, r_1)/r_1]|_{y=1} \qquad (3.21)$$

where B_n' s are constants given in equation (3.20). The differences between the wave function products of hydrogen 1s and 2s (equations 3.6 and 3.21) are the multiple coefficients and the order of n. The nature of the differentiable function equation (3.21) in the present case is similar to that of equation (3.6) in ESGH process .

The interaction V_d is same as given in the ESGH process. Substitution of the equations (3.7 and 3.21) in the scattering amplitudes equations (2.12, 2.57, 2.36, 2.43) we obtain the corresponding contributions to the DCS equation (3.2). These scattering amplitudes are given as

$$f^{(1)}_{i\to f} = -\frac{1}{2\pi}\iint d\underline{r}_o\, d\underline{r}_1\; \Psi_i(r_1)\left[-\frac{1}{r_o} + \frac{1}{|\underline{r}_o - \underline{r}_1|}\right] \Psi^*_f(r_1)\exp(i\,\underline{q}.\underline{r}_o)$$

$$= -\frac{1}{2\pi}\iint (B^2 + 2ABr_1 + A^2 r_1^2)\left[-\frac{1}{r_o} + \frac{1}{|\underline{r}_o - \underline{r}_1|}\right]\exp(i\,\underline{q}.\underline{r}_o)\exp(-y\,r_1)\, d\underline{r}_o\, d\underline{r}_1$$

$$= 16\pi\left[B^2 - 2ABD^1(y) + A^2D^2(y)\right]\frac{(q^2+2y^2)}{y^3(q^2+y^2)^2}$$

$$= \sum_{n=o}^{2} A_n \; D^n(y) \left[\frac{(q^2 + 2y^2)}{y^3(q^2 + y^2)^2} \right] \Big|_{y=1} \qquad (3.22)$$

where $A_o = 2$, $A_1 = 2$ and $A_2 = 0.5$, D^o represents the case without differentiation. The closed form of the first Born term (equation 3.22) in the ESEH process is similar to that of (equation 3.8) in ESGH process.

Now the imaginary part of the second Born term can be obtained by analogy of the results of the ESGH process (equations 3.9, 3.10, 3.11). The imaginary part in the present process is

$$\mathrm{Im}\; f^{(2)}_{HEA} = -\frac{4}{k_i} \sum_{n=1}^{3} B'_n \, D^n(y) \int \frac{d\underline{p}}{(|\underline{q} - \underline{p}|^2 + \beta_i^2)\, y^2}$$

$$\left[\frac{2}{(p^2 + \beta_i^2 + y^2)} - \frac{q^2}{(q^2 + y^2)(p^2 + \beta_i^2)} \right]$$

.....(3.23)

The two dimensional $\underline{p}$ integral procedure is given in the appendix. The closed form of the equation (3.23) can be obtained as

$$\mathrm{Im}\; f^{(2)}_{HEA} = -\frac{1}{k_i} \sum_{n=1}^{3} B_n \; D^n(y) \frac{1}{y^2} [\, 2\, I_1(\beta_i^2, y^2) -$$

$$\frac{q^2}{(q^2 + y^2)} \; I_1^{1'}(\beta_i^2 \, , \, 0) \;] \qquad (3.24)$$

where $I_1 (\beta_i^2 , y^2)$ is a function of β_i^2 , q^2 and y^2 and $I_1' (\beta_i^2 , 0)$ is only function of q^2 and β_i^2 . The integral form of these functions is given as

$$I_1 \; (\beta_i^2 , y^2) = \int \frac{d\underline{p}}{(|\underline{q} - \underline{p}|^2 + \beta_i^2) (p^2 + \beta_i^2 + y^2)}$$

and

$$I_1' (\beta_i^2 , 0) = I_1 (\beta_i^2 , y^2) \Big|_{y=0}$$

The solutions of these integrals are given in the ESGH process (under equation 3.11). Now the coefficients in the scattering amplitude (equation 3.24) are

$$B_1 = 0.159 \, , \qquad B_2 = 0.159, \qquad B_3 = 0.0398 \, .$$

Now following the same procedure, we will obtain the real part (equation 2.58) of the second Born term using the results of equation (3.13) and the product of the wave function (equation 3.21). This real part contribution to the DCS can be given as

$$\mathrm{Rel}\ f^{(2)}_{HEA} = \frac{4}{k_i \pi} \sum_{n=1}^{3} B_n' \ D^n(y)\ \mathcal{P} \int d\underline{p} \int_{-\infty}^{\infty} \frac{dp_Z}{(p_Z - \beta_i)}$$

$$\frac{1}{y^2(|\underline{q} - \underline{p}|^2 + p_Z^2)} \left[\frac{2}{(p^2 + p_Z^2 + y^2)} - \right.$$

$$\left. \frac{q^2}{(p^2 + p_Z^2)(q^2 + y^2)} \right] \quad (3.25)$$

The evaluation of the principal value integral, dp_Z is same as discussed in the ESGH process. The closed form of this (equation 3.25) is similar to that of the real part (equation 3.13).

$$\mathrm{Rel}\ f^{(2)}_{HEA} = \frac{1}{\pi k_i} \sum_{n=1}^{3} B_n \ D^n(y) \frac{1}{y^2} \left[2\, I_2(\beta_i^2, y^2) - \right.$$

$$\left. \frac{q^2}{(q^2 + y^2)} I_2'(\beta_i^2, 0) \right] \quad (3.26)$$

The constants B_n' s in this amplitude are same as in imaginary amplitude (equation 3.24). Here also $I_2(\beta_i^2, y^2)$ is function of q^2, β_i^2, and y^2, and $I_2'(\beta_i^2, 0)$ is function of q^2 and β_i^2. The integral representation of these functions are given below and the solutions of these are given previously (under equation 3.13).

$$I_2(\beta_i^2, y^2) = \mathcal{P} \int_{-\infty}^{\infty} \frac{d\underline{p} \quad dp_Z}{(p_Z - \beta_i)\,(\,|\underline{q} - \underline{p}\,|^2 + p_Z^2)(p^2 + p_Z^2 + y^2)}$$

$$I_2'(\beta_i^2, 0) = I_2'(\beta_i^2, y^2)\Big|_{y=0}$$

By a carefull analysis and comparison of the derived scattering amplitudes (equations 3.8, 3.22, 3.11, 3.24 , 3.13 and 3.26) in the ESGH and ESEH processes, we can obtain the real part (equation 2.59) in the closed form through the equations (3.21, (3.14) is given as

$$\mathrm{Re}2\, f^{(2)}_{HEA} = \frac{1}{2\,\pi\, k_i^2} \sum_{n=1}^{3} B_n\, D^n(\,y\,)\, D'\Big[\, \frac{I_3'(\beta_i, 0)}{(\,q^2 + y^2)} + \frac{I_3(\beta_i, y)}{y^2} - I_2(\beta_i^2, y^2)\Big] \qquad \ldots\ldots\ldots(3.27)$$

where the constants B_n's and the closed form of the functions in the above equation are given previously. The integral form of the function $I_3(\beta_i, y)$ is

$$I_3(\beta_i, y) = \mathcal{P} \int d\underline{p} \int_{-\infty}^{\infty} \frac{dp_Z}{(p_Z - \beta_i)\,(p^2 + p_Z^2 + y^2)}$$

and $I_3'(\beta_i, 0) = I_3(\beta_i, y)\big|_{y=0}$

The analysis of the GES term (equation 2.45) in this ESEH process is similar to that of the ESGH (equation 3.16). The third GES term (equation 3.16) was given for a typical wave function of the type '' $A^2 \exp(-y\, r_1)$ '' . By the substitution of $y = 2$ we got the amplitude corresponding to ESGH process. The reformulated equation (3.16) can be used here to obtain the GES in the present case. The closed form of this which can be obtained through the equations (2.45, 3.16 , 3.20), is given as

$$f^{(3)}_{GES} = -\frac{y^4 \pi}{16\, k_i^2} \sum_{n=1}^{3} B_n' \, D^n(y)\, F(q, y)$$

$$= -\frac{\pi}{16\, k_i^2} \sum_{n=1}^{3} C_n \, D^n(y)\, F(q, y)\Big|_{y=1} \qquad \ldots\ldots (3.28)$$

where $F(q, y)$ is a function of q and y which was given in the ESGH process (equation 3.16). And the constants C_n' s are obtained as $C_1 = 0.0398$, $C_2 = 0.0398$ and $C_3 = 0.00995$.

In the final stage of this ESEH process we derive the expression for the first order exchange scattering amplitude through the Ochkur , (1963) approximation. This exchange scattering amplitude can be obtained easily from the equation (3.17) . Now substituting the product of the wave function (equation 3.20) in the integral form of equation (3.17) we will obtain this exchange contribution as follows.

$$g_{och} = -\frac{2}{k_i^2} \int d\,\underline{r}_1 \; \exp(\, i\, \underline{g}.\underline{r}_1 \,) \,(B^2 + 2\, ABr_1 + A^2 r_1^2 \,) \; \exp(\, -y\, r_1 \,)$$

$$= -\frac{2}{k_i^2} \int \sum_{n=0}^{2} B_n' \; D^n(\, y \,) \exp(\, i\, \underline{g}.\underline{r}_1 \,) \; \exp(\, -y\, r_1 \,) \; d\,\underline{r}_1$$

$$= -\frac{2}{k_i^2} \sum_{n=0}^{2} B_n' \; D^n(\, y \,) \int \exp(\, i\, \underline{g}.\underline{r}_1 \,) \; \exp(\, -y\, r_1 \,) \; d\,\underline{r}_1$$

By analogy of the expression (equation 3.17) we can write the solution of the above integral as

$$= - \frac{16\pi}{k_i^2} \sum_{n=0}^{2} B_n' \, D^n(y) \left[y \left(q^2 + y^2 \right)^{-2} \right]$$

$$g_{och} = - \frac{1}{k_i^2} \sum_{n=0}^{2} A_n \, D^n(y) \left[y \left(q^2 + y^2 \right)^{-2} \right] \Big|_{y=1}$$

..... (3.29)

where A_n' s are constants defined in equation (3.22).

3.3.2 Comparison of present ESEH results with the other theoretical results :

Similar to ESGH process, we have calculated DCS, TCS using the HHOB scattering contributions equations (3.22, 3.24, 3.26, 3.28, 3.29) at incident energies 100 to 700 eV and in the angular range $\theta \leq 120^{\circ}$. We used an average excitation energy DE = 0.05556 a.u (Joachain et al , 1977b) in the calculation of the second Born term (equations 3.24, 3.26, 3.27). The present ESEH results (DCS, TCS) are listed in the Tables (3.8, 3.9 and 3.4). And the DCS at incident energies E = 200 and 400 eV are shown graphically along with the other theoretical results. Unfortunately so far no experimental data was available for comparison. As it was mentioned very less attention was paid by our pioneer workers to study this type of ESEH process. A large

deviation of DCS was observed from one approximation to another approximation in this process. As in the case of ESGH here also we observed that the present DCS agrees well with compared EBS results in the angular range $\theta \leq 50^{\circ}$, which is a direct checking of our calculations.

Fig. (3.3) shows the two sets of results with the present DCS (solid curves a and b) along with the recent theoretical results. The meaning of curves a and b was same as given in Fig. (3.1). In set A the present DCS at incident energy E = 200 eV are compared with the theoretical results, + — EBS results of Joachain et al, (1977b), ▲ — simplified second Born approximation of Joachain et al, (1977a), O —TPE (Two - potential eikonal) approximation results of Pundir et al, (1982). In set B the present DCS at incident energy E = 400 eV are compared with , ------- static approximation results of Joachain et al, (1977b), • — OM (Optical Model) results of Joachain et al, (1980). The rest of the representations in this set B are same as in set A .

It was observed from the Fig. (3.3) that the effect of rest part (equation 3.27) is very less at 400 eV than at 200 eV in the angular region $\theta \leq 25^{\circ}$. This was

also observed in ESGH process (not given specifically, but can be identified from Table 3.1). And the exchange contribution to DCS is almost negligible over the entire angular region (specifically given by Rao and Desai, 1983a) in this ESEH process. In anticipation of experimental data in the near future and according to our ESGH analysis, we are expecting that the present DCS will give good comparison in the angular range $\theta \lesssim 50^{o}$.

The description of the Table (3.8) was same as Table (3.1). This Table (3.8) shows all the scattering amplitudes (equations 3.26, 3.27, 3.28, 3.29, 3.24) in the ESEH process at incident energies E = 200 and 400 eV . In the Table (3.9) we have listed the DCS (without exchange) in the energy region $E \doteq 100 - 700$ eV, over the angular range $\theta \lesssim 60^{o}$. In this table at each angle θ , and energy E, two DCS results are given, corresponding to the inclusion of real part (equation 3.27) of $O (k_i^{-2})$ (higher DCS) and exclusion of this real part (equation 3.27) (lower DCS) in the DCS (equation 3.2) calculation. Table (3.4) shows the present ESEH , TCS in the energy range 100 to 700 eV. The ratios of ESEH, TCS to the TCS of ESGH process are also listed in this Table (3.4).

From the Table (3.8) it was observed that the exchange contribution (equation 3.29) to the DCS (equation 3.2) is negligible over the entire angular range. And Table (3.9) shows that the effect of real part (equation 3.27) in the DCS is more as Θ increases (for a particular incident energy), and is less as incident energy increases (for a particular scattering angle Θ) . These variations reveal the poor convergence of (equation 3.27) at large moment transfer (q) (fixed k_i) and good convergence at higher incident energies (fixed Θ) respectively. This was the reason for the considerable separation observed between the curves a and b (Figs. 3.1 and 3.3) . The ratios of TCS's for ESEH and ESGH are observed ranging nearly from 20 to 18 at incident energies 100 to 700 eV respectively (this type of observation was noted previously by Pundir et al , 1982).

The results obtained in ESGH and ESEH are very encouraging in the angular region $\Theta \leq 60^{o}$ and at incident energies E = 100 to 700 eV. The first order exchange effects to the DCS are found more in ESGH than in ESEH process. The ESGH results can be improved further by the inclusion of higher order exchange terms (Sec. 2.3.1). We will deal this point in the last section of this chapter. With the success of these elastic

processes, we would like to extend the present approximations to the inelastic scattering process.

3.4.1 <u>Inelastic scattering of electrons by hydrogen atom</u> (ISH) :

(Desai and Rao, 1983a)

$$\bar{e} + H(1s) \longrightarrow \bar{e} + H^{*}(2s) \qquad (3.30)$$

Most of the experimental evidences on this process refer to the excitation of the 2s and 2p states. TCS have been measured by looking at radiation emitted from atoms following excitation, both for the 2p state (Long et al, 1968) and the 2s state (Kaupilla et al, 1970). Very recently absolute angular distributions of scattered electrons have been measured by Williams and Willis (1975). Since the 2s and 2p states are degenerate Williams and Willis were able to determine only the sum of the 2s and 2p differential cross sections by looking at the energy loss spectra.

The theoretical picture is complicated than for ESGH (Sec. 3.2.1) process , due to the asymmetry of the initial and final wave functions. The results obtained in the HHOB approximation (Sec. 2.3.4) can be valid for the inelastic processes

In this ISH process (equation 1.2) the final state of the target atom (H^* (2s)), equation (3.19) is different than the initial state (H (1s)), equation (3.5). And the momentum transfer $\underline{q}$ to the target during this collission process is

$$\underline{q} = \underline{k}_i - \underline{k}_f$$

$$|\underline{q}|^2 = |\underline{k}_i - \underline{k}_f|^2$$

$$q^2 = k_i^2 + k_f^2 - 2\, k_i\, k_f \cos\theta \qquad (3.31)$$

here $k_i \neq k_f$ and the value of k_f can be calculated using the energy conservation. This final momentum of the scattered electron can be given as

$$k_f = (k_i^2 - 3/4)^{1/2} \qquad (3.32)$$

The initial and final wave functions (equations 3.5 and 3.19) of the hydrogen are given as

$$\Psi_{1s}(r_1) = \frac{1}{\pi^{1/2}} \exp(- r_1) \qquad (3.33)$$

$$\Psi_{2s}(r_1) = \frac{1}{4(2\pi)^{1/2}} (2 - r_1) \exp(- r_1 /2) \qquad \ldots. (3.34)$$

and the product of these wave functions can be written in differentiation form

$$\therefore \psi^*_{2s}(r_1)\,\psi_{1s}(r_1) = -\sum_{n=1}^{2}\left[A'_n D^n(y)\right.$$
$$\left.\exp(-y\,r_1)/r_1\right]\Big|_{y=1.5} \qquad (3.35)$$

where the constants A'_n s can be obtained from the equations (3.33, 3.34). Substituting the equations (3.7) and (3.35) in the scattering amplitudes (equations 2.12, 2.57, 2.36, 2.43) we can obtain the corresponding scattering amplitudes for ISH processes follows.

The first Born inelastic amplitude can be derived through the equations (3.35) and (3.22).

$$f^{(1)}_{i\to f} = \sum_{n=0}^{1} A_n D^n(y)\left[\frac{(q^2+2y^2)}{y^3(q^2+y^2)^2}\right]\Big|_{y=1.5} \qquad (3.36)$$

where $A_0 = 5.65685$, $A_1 = 2.92843$ are constants. The imaginary part of second Born for ISH can be obtained from the equations (3.24) and (3.35).

$$\mathrm{Im}\ f^{(2)}_{HEA} = -\frac{1}{k_i}\sum_{n=1}^{2} B_n D^n(y)\,\frac{1}{y^2}\left[H_1(q,\beta_i,y)\right]$$
$$\ldots\ldots.(3.37)$$

where $B_1 = 0.45016$, $B_2 = 0.22508$, and $H_1(q,\beta_i,y)$ is a differentiable function, similar to that of corresponding square bracket terms in equations(3.11), (3.24). In the similar way the remaining scattering amplitudes which can be obtained from equations (3.26, 3.27, 3.28) and (3.35) are given as

$$\mathrm{Re1}\ f^{(2)}_{HEA} = \frac{1}{\pi k_i} \sum_{n=1}^{2} B_n D^n(y) \frac{1}{y^2} [H_2(q,\beta_i,y)] \quad \ldots (3.38)$$

$$\mathrm{Re2}\ f^{(2)}_{HEA} = \frac{1}{2\pi k_i^2} \sum_{n=1}^{2} B_n D^n(y) D' [H_3(q,\beta_i,y)] \quad \ldots (3.39)$$

and

$$f^{(3)}_{GES} = -\frac{\pi}{16 k_i^2} \sum_{n=1}^{2} C_n D^n(y) [F(q,y)] \quad (3.40)$$

Here the square bracket functions are similar to that of the respective scattering amplitudes in ESGH and ESEH (Secs. 3.2.1 , 3.3.1) processes . And the constants in (equation 3.40) are obtained as $C_1 = 0.56973$, $C_2 = 0.28487$. First order exchange term can be derived easily for the present ISH process, using the ESGH, ESEH expressions (equations 3.17, 3.29).

3.4.2 Comparison of present ISH results with the other theoretical results :

Similar to ESGH and ESEH processes, here also we have calculated DCS at incident energies E = 100 to 700 eV, over the angular region $\theta \leq 120^{\circ}$. HHOB scattering amplitudes equations (3.36, 3.37, 3.38, 3.39, 3.40) are used in these calculations. In order to study

the sensitivity of DCS and real part (equation 3.39) with respect to the choice of the excitation energy DE , we have performed the detailed calculation of DCS and second Born term (equations 3.37, 3.38, 3.39) at two different excitation energies , DE = 0.375 a.u and DE' = 0.250 a.u (Byron and Latour, 1976). And these results are presented in the Tables (3.5 to 3.7). In Table (3.7) we have given recent theoretical results along with the present DCS . And the results at incident energies E = 100 to 300 eV are shown in Figs. (3.4 to 3.6). Satisfactory agreement was observed when the present results were compared with other results .

Fig. (3.4) shows two sets of results with the present DCS (solid curves a' and b') along with the recent theoretical results. Set A (Fig. 3.4A) shows the present DCS (calculated using DE = 0.375) at incident energy E = 100 eV, over the angular range $\theta \leq 30^{o}$. These results are compared with the recent theoretical results, ▲— CCSOPM (Coupled - Channel Second Order Potential Model) of Bransden et al (1982), --------- — of Unnikrishnan and Prasad (1982) and ● — results of Glouber (1959). Set B (Fig. 3.4B) shows the present DCS at incident energy E = 200 eV.

The compared results are same as in Fig.(3.4A). The DCS results are found in good agreement at incident energy E = 200 eV than at 100 eV.

Fig. (3.5) shows the present imaginary part (equation 3.37, with DE = 0.375) (solid curve) at incident energy E = 100 eV. This imaginary part ~~was~~ is compared with that of Byron and Latour (1976) (solid circles). This comparison was a direct checking of our calculations.

Fig. (3.6) shows two sets of results with the present DCS (solid curve a') and the experimental results. Set A shows present DCS at incident energy E = 200 eV, and the experimental data • — of Williams (1975) (for n=2). Set B shows same comparison as set A, at incident energy E = 300 eV. These comparisons are made only to show that the present DCS are within the limits of experimental data.

In Table (3.5) we have listed the ISH amplitudes (equations 3.37, 3.38, 3.39, 3.40) calculated with DE = 0.375 and DE' = 0.250 , these amplitudes are given (denoted without and with prime respectively) at incident energies E = 100 and 400 eV. Table (3.6) shows the present DCS in the incident energy range E = 100

to 700 eV. It was noted from the Tables (3.5 and 3.6) that considerable variation was observed in the scattering amplitudes for a difference of 0.125 in the excitation energy, over the angular range $\Theta \leq 60^{o}$. Real parts (equations 3,38, 3.39) are more effective than imaginary part (equation 3,37) for this difference of excitation energy. Correspondingly variation was observed in the DCS . In Table (3.7) we have compared our DCS at incident energies E = 100 and 200 eV, with the recent theoretical results (Bransden et al, 1982 ; Kingston et al, 1976). Satisfactory agreement was noted in these comparisons.

Finally it was noted from the Figs. (3.4 to 3.6) and Tables (3.5 to 3.7), that the present results are satisfactory, and within the limits of theoretical and experimental comparisons . And the choice of excitation energy was important in the ISH process . Second Born term was very sensitive for the excitation energy. The variation of DCS (for DE = 0.375 a.u , DE' = 0.250 a.u) was negligible at higher incident energies than at lower incident energies.

After this ISH process we would like to study the exact DCS with higher order exchange terms. This idea was introduced in the Sec. (3.3.2) for the improvement of ESGH process results (Sec.3.2.2).

3.5.1 <u>Born exchange amplitudes for ESGH process</u> :

(Desai and Rao, 1982)

$$\bar{e}\,(\,r_1\,) + H\,(\,r_1\,) \longrightarrow H\,(\,r_2\,) + \bar{e}\,(\,r_1\,) \qquad .....(3.41)$$

Until now we have restricted our attention to collisions [ISH (Sec. 3.4.1), ESEH (Sec. 3.3.1), ESGH (Sec.3.2.1)] in which all of the particles involved are distinct. Since the majority of interesting experiments do not satisfy this condition - electron - atom collisions involve several identical electrons, nucleon - nucleous collisions involve several identical nucleous and so on. There were several ways to set up a scattering theory of identical particles (Heep, 1965). The actual scattering states, properly symmetrized for the identical particles can be obtained from those of the distinguishable case(Chapter II) by using the appropriate symmetrizing projection operators. This in turn will mean that the scattering amplitudes for identical particles (identified by $\bar{F}$) can be expressed as sum or differences of certain related amplitudes for distinct particles. Thus, it follows that all of the approximations (Chapter II) for distinct particles can be immediately applied to the identical particle problem. As an example the exact scattering amplitude for ESGH process (Sec. 3.2.1) can be given as

$$\bar{F}(P' \leftarrow P) = f^{d}_{ba}(P' \leftarrow P) - g^{ex}_{ba}(P' \leftarrow P) \quad \ldots.(3.42)$$

Here first term of right side is the direct amplitude (equation 2.33, and Sec. 2.3.1) for the incident electron - treated as distinct from that in the target atom (ESGH, Sec. 3.2.1) to scatter elastically with momentum P', and the second term is the exchange amplitude (equation 2.36) (approximated as g_{och} in Sec. 3.2.1) for the process in which the target electron is ejected with momentum P', while the incident electron is captured. Since the electrons are indistinguishable in reality, these two processes cannot be apart, and since the electrons are Fermions, the appropriate observed amplitude is the difference of the two amplitudes (equation 3.42).

The exchange scattering amplitude (equation 2.36) was approximated through the first order term (equation 3.17) using Ochkur (1963) approximation, for the consistent expansion of the DCS (equation 3.2), O (k_i^{-2}) in atomic hydrogen (Sec. 3.2.1). This approximate exchange amplitude may not given (Byron and Joachain , 1977) leading contribution of the exchange amplitude.

In the present study we made an attempt to derive the second term of the exchange amplitude (equation 2.36)

using the HEA (Sec. 2.3.5) and Ochkur (1963) approximations for the ESGH process (Sec. 3.2.1).

The second Born approximation (equation 2.57) for the direct scattering process was given as

$$f^{(2)}_{HEA} = \frac{i}{2\pi k_i} \int d\underline{r}_o \exp (i \underline{q}.\underline{r}_o) < \psi_f | V_d (\underline{r}_o .. \underline{r}_z)$$

$$- \int_{-\infty}^{\infty} dZ_o' \; H (Z_o') \exp (- i \beta_i Z_o')$$

$$[V_d (\underline{r}_o - Z_o' \hat{y} \; ; \; \underline{r}_1 \ldots, \underline{r}_z) + \frac{i Z_o'}{2 k_i}$$

$$D^2_{r_o'} V_d (\underline{r}_o - \underline{r}_o' , \underline{r}_1 \ldots \underline{r}_z)] | \psi_i > |_{b_o'} = 0$$

....(3.43)

Now the second Born exchange amplitude can be obtained from the equation (2.37) as

$$\bar{g}_{B2} = - (2\pi)^2 < \Phi_{pb} | V_p \; G^{(+)}_d \; V_d | \Phi_a > \qquad (3.44)$$

Taking the permutation of the electron and target wave functions in the final channel, we will obtain (equation 3.44) in HEA (Sec. 2.3.5). Now the second Born exchange amplitude of $O (k_i^{-1})$ (equation 3.44) for hydrogen atom can be obtained from (equation 3.43), given as

$$g^{(2)}_{HEA} = \frac{i}{2\pi^2 k_i} \int d\underline{r}_o \exp (i \underline{k}_i \cdot \underline{r}_o - y_o r_o) V_p (\underline{r}_o , \underline{r}_1)$$

$$- \int_{-\infty}^{\infty} dZ_o' H (Z_o') \exp (- i \beta_i . Z_o') V_d$$

$$(\underline{r}_o - Z_o' \hat{y} , \underline{r}_1)$$

$$\int d \underline{r}_1 \exp (- i \underline{k}_f \cdot \underline{r}_1 - \hat{y}_1 r_1) \qquad (3.45)$$

where $y_o = y_1 = 1$, and $V_p (\underline{r}_o , \underline{r}_1)$ is the interaction between the incident electron and target hydrogen in the rearranged channel. This interaction can be obtained taking the permutation of V_d (equation 3.7) in the initial channel .

$$V_p (\underline{r}_o , \underline{r}_1) = - \frac{1}{r_1} + \frac{1}{| \underline{r}_o - \underline{r}_1 |} \qquad (3.46)$$

substituting the fourier form of the interactions for $V_p (\underline{r}_o , \underline{r}_1)$ and $V_d (\underline{r}_o - Z_o' \hat{y} , \underline{r}_1)$ through equations (2.52, 2.53) in (3.45) , it will reduce to

$$g^{(2)}_{HEA} = \frac{i}{2\pi^2 k_i} \int d \underline{r}_o \exp (i \underline{k}_i \cdot \underline{r}_o - y_o r_o)$$

$$\int d \underline{K} [\exp (i \underline{K} \cdot \underline{r}_o) - 1]$$

$$\frac{\exp (- i \underline{K} \cdot \underline{r}_1)}{2 \pi^2 K^2}$$

$$\int d\,\underline{r}_1 \;\exp(-i\,\underline{K}_f\cdot\underline{r}_1 - y_1\,r_1)\int_{-\infty}^{\infty} dZ_o'\,H(Z_{1o}')$$

$$\exp(-i\,\beta_i\,Z_o')$$

$$\frac{1}{2\pi^2\,(p'^2+p_Z'^2)}\int_{-\infty}^{\infty} d\,p_Z'\;\exp i\,(-p_Z'\,Z_o + p_Z'\,Z_o')$$

$$\int d\underline{p}'\;\exp(i\,\underline{p}'\cdot\underline{b}_o)\,[\exp(i\,\underline{P}'\cdot\underline{r}_1) - 1] \qquad (3.47)$$

(where $\underline{P}' = \underline{p}' + p_Z'\,\hat{y}$) .

After the evaluation of dZ_o' integral (given in Sec. 2.3.5) the real and imaginary parts of the equation (3.47) can be separated as

$$\mathrm{Re}\;g^{(2)}_{HEA} = \frac{-1}{8\pi^6\,k_i}\,\mathcal{P}\int_{-\infty}^{\infty}\frac{dp_Z'}{(p_Z' - \beta_i)}\,[\int d\,\underline{r}_o$$

$$\exp(i\,\underline{k}_i\cdot\underline{r}_o - y_o\,r_o)\int d\,\underline{K}\;\exp(-i\,\underline{K}\cdot\underline{r}_1)$$

$$[\exp(i\,\underline{K}\cdot\underline{r}_o) - 1]\;\frac{1}{K^2}\int d\,\underline{r}_1$$

$$\exp(-i\,\underline{k}_f\cdot\underline{r}_1 - y_1\,r_1)\int d\underline{p}'\;\exp(-i\,\underline{p}'\cdot\underline{b}_o)$$

$$[\exp(i\,\underline{p}'\cdot\underline{b}_1 + i\,p_Z'\,Z_1) - 1]\;\frac{1}{(p'^2 + p_Z'^2)}\;]$$

.....(3.48)

$$\mathrm{Im}\ g^{(2)}_{HEA} = \frac{i}{8\,\pi^5\,k_i}\ [\ \int\!\!\_\_\_\_\_\ \int\!\!\_\_\_\_\_\ \int\!\!\_\_\_\_\_\ \int\!\!\_\_\_\_\_$$

$$[\ \exp\,(i\ \underline{p}'\cdot\ \underline{b}_1 + i\ \beta_i Z_1) - 1]\ \frac{1}{(p'^2 + \beta_i^2)}\ ]$$

.... (3.49)

The p_Z' variable in real part (equation 3.48) is replaced by β_i in the imaginary part (equation 3.49) (See equations 2.58, 2.60). First we consider the integral evaluation of imaginary part, because these results can be easily extended to real part integrals. From equations (3.48) and (3.49) the imaginary part equation (3.49) can be written as

$$\mathrm{Im}\ g^{(2)}_{HEA} = \frac{i}{8\,\pi^5\,k_i}\ \int d\underline{r}_o\ \exp\,(\ i\ \underline{k}_i\cdot\underline{r}_o - y_o\ r_o\ )$$

$$\int \frac{d\underline{K}}{K^2}\ \int \frac{d\,\underline{p}'}{(p'^2 + \beta_i^2)}\ \int d\underline{r}_1\ \exp(-i\ k_f\cdot r_1 - y_1 r_1)$$

$$[\ \exp\,(\ -\ i\ (\ \underline{K} - \underline{P}')\cdot(\ \underline{r}_1 - \underline{r}_o\ ) - 1$$

$$\exp\,(\ -\ i\ \underline{K}\ \cdot(\ \underline{r}_1 - \underline{r}_o\ ) - i\ \underline{P}'\cdot\ \underline{r}_o\ ) -$$

$$\exp\,(\ -\ i\ \underline{K}\ \cdot\ \underline{r}_1 + i\ \underline{P}'\cdot\ (\ \underline{r}_1 - \underline{r}_o\ )\ ) +$$

$$\exp\,(-i\ (\ \underline{K}\ \cdot\ \underline{r}_1 + \underline{P}'\cdot\ \underline{r}_o\ )\ )\ ] \qquad (3.50)$$

$$= \frac{i}{8\,\pi^5\,k_i} \int d\underline{r}_o \exp\left(i\,\underline{k}_i \cdot \underline{r}_o - y_o\, r_o \right) \int \frac{d\underline{K}}{K^2}$$

$$\int \frac{d\underline{p}'}{(p'^2 + \beta_i^2)} \int d\underline{r}_1 \exp\left(- i\,\underline{k}_f \cdot \underline{r}_1 - y_1\, r_1 \right)$$

$$[\ A - B - C + D\ ] \qquad (3.51)$$

where A, B, C and D are the respective exponential terms in equation (3.5o) . Now consider the integrals with the first term (A) of equation (3.51).

$$\frac{i}{8\,\pi^5\,k_i} \int \frac{d\underline{p}'}{(p'^2 + \beta_i^2)} \int \frac{d\,\underline{K}}{K^2} \int d\underline{r}_o \exp\left(- y_o\, r_o \right)$$

$$\exp\left(i\,(\underline{K} - \underline{P}' + \underline{k}_i) \cdot \underline{r}_o \right) \int d\underline{r}_1 \exp\left(- y_1\, r_1 \right)$$

$$\exp\left(- i\,(\underline{K} - \underline{P}' + \underline{k}_f) \cdot \underline{r}_1 \right)$$

$$= \frac{8\,i}{\pi^3\,k_i} \int \frac{d\underline{p}'}{(p'^2 + \beta_i^2)} \int \frac{d\underline{K}}{K^2}$$

$$\frac{1}{\left(y_o^2 + |\underline{K} - \underline{P}' + \underline{k}_i|^2 \right)^2 \left(y_1^2 + |\underline{K} - \underline{P}' + \underline{k}_f|^2 \right)^2}$$

Substituting , $\underline{Q} = \underline{K} - \underline{S}$ and $\underline{S} = \underline{P}' - \underline{k}_i$ in the above integral

$$= \frac{8\,i}{\pi^3\,k_i} \int \frac{d\underline{p}'}{(p'^2 + \beta_i^2)}$$

$$\int \frac{d\,\underline{Q}}{(\underline{Q} + \underline{S})^2\,(y_o^2 + Q^2)^2\,(y_1^2 + |\,\underline{Q} + \underline{q}\,|^2)^2}$$

in the large incident energy region (Ochkur, 1963) this integral can be written as

$$= \frac{8\,i}{\pi^3\,k_i} \int \frac{d\,\underline{p}'}{(p'^2 + \beta_i^2)\,(|\,\underline{P}' - \underline{k}_i\,|^2)}$$

$$\int \frac{d\,\underline{Q}}{(1 + Q^2)^2\,(1 + |\,\underline{Q} + \underline{q}\,|^2)^2}$$

using the integral techniques (Gradshteyn and Ryzhik, 1965; Joachain , 1975) for the evaluation of $d\,\underline{Q}$, we will obtain this as

$$= \frac{16\,i}{\pi\,k_i\,(q^2 + 4)^2} \int \frac{d\,\underline{p}'}{(p'^2 + \beta_i^2)\,(|\,\underline{P}' - \underline{k}_i\,|^2)}$$

$$= \frac{16\,i}{\pi\,k_i\,(q^2 + 4)^2} \int_o^\infty$$

$$\int_o^{2\pi} \frac{p'\,d\,p'\,d\,\phi'}{(p'^2 + \beta_i^2)\,(p'^2 + \beta_i^2 + k_i^2 - 2\,k_i\beta_i)}$$

The integral procedure for $d\,\underline{p}'$ (given in appendix) is similar to that of $I_1\,(\beta_i^2\,,\,y^2)$ integral in the ESGH process (Sec. 3.2.1) and denoting the final closed form of the above as E1

$$E1 = \frac{32}{k_i^2\,(q^2+4)^2\,(k_i - 2\,\beta_i)} \log\left(\frac{k_i - \beta_i}{\beta_i}\right)$$

Similarly , the closed form of the integrals with the other terms (B, C, D) in equations (3.50, 3.51) can be obtained.

$$E_2 = -\frac{4}{\pi\,k_i^2\,(k_i - 2\,\beta_i)}\,D^1(y)\,[\,I_1(\beta_i^2\,,\,y^2) - I_1(u^2\,,\,v^2)\,]$$

$$E_3 = \frac{8}{\pi\,k_i}\,D^1(y')\,\frac{1}{y'^2}\,\left[\frac{1}{(k_i^2 - 2\,k_i\,\beta_i + y'^2)}\log\left(\frac{(y'^2 + (k_i - \beta_i))^{1/2}}{\beta_i}\right) - \frac{1}{k_i\,(k_i - 2\,\beta_i)}\log\left(\frac{k_i - \beta_i}{\beta_i}\right)\right]$$

$$E_4 = -\frac{8}{\pi k_i^3} D^1(y')\left[\frac{1}{(k_i^2 - 2k_i\beta_i + y'^2)}\right.$$

$$\left.\log\left(\frac{(y'^2 + (k_i - \beta_i)^2)^{1/2}}{\beta_i}\right)\right]$$

where $y = 2$, $u^2 = \beta_i^2 + y^2$; $v^2 = (k_i - \beta_i)^2$, $y' = 1$

$$\therefore \quad \mathrm{Im}\ g^{(2)}_{HEA} = E1 - E_2 - E_3 + E_4 \qquad (3.52)$$

The integral form of $I_1(\beta_i^2, y^2)$, $I_1(u^2, v^2)$, and the solutions of these integrals are similar to those given in ESEH (Sec. 3.3.1) and ESGH (Sec. 3.2.1) processes. The TCS (equation 3.3) corresponding to the exchange amplitude (equation 3.52) can be obtained in the forward direction ($q = 0$).

$$\sigma^{ex}_{tot} = \frac{4\pi}{k_i} \mathrm{Im}\ g^{(2)}_{HEA}(0) \qquad (3.53)$$

This exchange correction (equation 3.53) is included to the direct TCS (equation 3.12). These results are given in the Table (3.4).

The real part exchange amplitude (equation 3.48) can be expressed in a similar way of imaginary part (equations 3.50, 3.51).

$$\mathrm{Re}\ g^{(2)}_{HEA} = -\frac{1}{8\pi^6 k_i} \mathcal{P} \int_{-\infty}^{\infty} \frac{dp'_Z}{(p'_Z - \beta_i)} \int d\underline{r}_o \text{ -----}$$

$$\int \frac{d\underline{K}}{K^2} \int \frac{d\underline{p}'}{(p'^2 + p'^2_Z)} \int d\underline{r}_1 \text{ ----}$$

$$[\ A - B - C + D\ ] \qquad (3.54)$$

Here A, B, C and D represent the first, second, third and fourth, exponential terms in the square bracket of equation (3.50) with $\underline{P}' = \underline{p}' + p'_Z\ \hat{y}$. The computation of the integrals $d\underline{r}_o$, $d\underline{r}_1$ and $d\underline{K}$ is similar to that of imaginary part (equation 3.50) . Consider the integrals (equation 3.54) with a typical term A.

$$\frac{-1}{8\pi^6 k_i} \mathcal{P} \int_{-\infty}^{\infty} \frac{d p'_Z}{(p'_Z - \beta_i)} \int \frac{d\underline{p}'}{(p'^2 + p'^2_Z)} \int \frac{d\underline{K}}{K^2} \int d\underline{r}_o$$

$$\exp(-y_o r_o)\ \exp(i(\underline{K} - \underline{P}' + \underline{k}_i) \cdot \underline{r}_o)$$

$$\int d\underline{r}_1 \exp(-y_1 r_1)\ \exp(-i(\underline{K} - \underline{P}' + \underline{k}_f) \cdot \underline{r}_1)$$

Using the old results of the integrals ($d\underline{r}_o$, $d\underline{r}_1$, $d\underline{K}$) given under equation (3.51) , we can ~~with~~ write this as

$$= \frac{-32}{\pi k_i (q^2 + 4)^2} \int_0^\infty p' \, dp' \, \mathcal{P} \int_{-\infty}^{\infty} \frac{dp_Z'}{(p_Z' - \beta_i)}$$

$$\frac{1}{(p'^2 + p_Z'^2)(p'^2 + (p_Z' - k_i)^2)}$$

$$= \frac{-32}{\pi k_i (q^2 + 4)^2} \int_{-\infty}^{\infty} p' \, dp' \, \mathcal{P} \int_{-\infty}^{\infty} \frac{dp_Z'}{(p_Z' - \beta_i)(k_i^2 - 2p_Z' k_i)}$$

$$\left[\frac{1}{p'^2 + p_Z'^2} - \frac{1}{p'^2 + (p_Z' - k_i)^2} \right]$$

$$= \frac{+32}{2 k_i^2 \pi (q^2 + 4)^2} \int_0^\infty p' \, dp' \, \mathcal{P} \int_{-\infty}^{\infty} \frac{dp_Z'}{(p_Z' - \beta_i)(p_Z' - a_1)}$$

$$\left[\frac{1}{p'^2 + p_Z'^2} - \frac{1}{p'^2 + (p_Z' - k_i)^2} \right]$$

$$= \frac{+16}{k_i^2 \pi (q^2 + 4)^2 (\beta_i - a_1)} \int_0^\infty p' \, dp' \, \mathcal{P} \int_{-\infty}^{\infty} dp_Z'$$

$$\left[\frac{1}{p_Z' - \beta_i} - \frac{1}{p_Z' - a_1} \right]$$

$$\left[\frac{1}{p_Z'^2 + p'^2} - \frac{1}{p'^2 + (p_Z' - \beta_i)^2} \right]$$

The closed form of the above integrals can be obtained by expanding the square bracket terms, and making use of the $I_3 (\beta_i , y)$ and $I_2 (\beta_i^2 , y^2)$ solutions given in appendix). Similar type of computation can be done for B, C and D terms in equation (3.54) . The final closed form of the equation (3.54) after the computation can be obtained as

$$\mathrm{Re}\ g^{(2)}_{HEA} = \frac{2}{(\beta_i - a_1)\,\pi\, k_i^2}\, D^1 (y)$$

$$[I_2 (\beta_i^2 , y^2) - I_2 (a_1^2 , y^2)] -$$

$$\frac{2}{\pi^2 k_i^2 (\beta_i - a_2)}\, D^1 (y') \frac{1}{y'^2}$$

$$[I_3 (y' , k_i - a_2) - I_3 (y' , k_i - \beta_i)] \qquad \ldots\ldots \quad (3.55)$$

where $a_2 = \frac{y'^2}{2k_i} + \frac{k_i}{2}$; $\qquad y' = 1$

$a_1 = \frac{k_i}{2}$; $\qquad y = 2$

The integral representations of $I_2 (a_1^2 , y^2)$ $I_3 (y' , k_i - a_2)$ in (equation 3.55) and the corresponding solutions are given in the appendix .

The first Born exchange amplitude can be obtained from (equation 2.37).

$$\bar{g}_{B1} = - \frac{1}{2\pi^2} \int d\,\underline{r}_o \; \exp\left(i\,\underline{k}_i \cdot \underline{r}_o - r_o \right) V_p \text{ or } V_d$$

$$\int d\,\underline{r}_1 \; \exp\left(- i\,\underline{k}_f \cdot \underline{r}_1 - r_1 \right)$$

$$= T_1 + T_2$$

where T_2 is the approximated first order term using the Ochkur , (1963) approximation for the electrostatic interaction term of V_d or V_p (equations 3.7, 3.46). And term T_1 corresponding to the nuclear interaction term of V_d . The final closed form of these two terms can be obtained as

$$\bar{g}_{B1} = \frac{16}{\left(k_i^2 + 1 \right)^3} - \frac{32}{k_i^2 \left(q^2 + 4 \right)^2} \qquad (3.56)$$

Now the exact scattering amplitude (equation 3.42) can be formulated using the direct (equations 3.8, 3.11 , 3.13, 3.15, 3.16) and exchange (equations 3.52, 3.55, 3.56) scattering contributions to the DCS for ESGH process (Sec. 3.2.1)

$$F_d = f^{(1)}_{i\to f} + \mathrm{Re1}\ f^{(2)}_{HEA} + \mathrm{Re2}\ f^{(2)}_{HEA} + f^{(3)}_{GES} + \mathrm{Im}\ f^{(2)}_{HEA} \qquad (3.57)$$

$$F_E = \bar{g}_{B1} + \mathrm{Re}\ g^{(2)}_{HEA} + \mathrm{Im}\ g^{(2)}_{HEA} \qquad (3.58)$$

$$EF = F_d \pm F_E$$

$$EDCS = |\ EF\ |^2 \qquad (3.59)$$

These cross sections are calculated at incident energies 100 to 700 eV , given in Table (3.2).

3.5.2 <u>Comparison of present ESGH</u> (included higher order exchange amplitudes) <u>results with the other data</u> :

Using the exchange scattering amplitudes (equations 3.51 , 3.55 , 3.56) and direct scattering amplitudes (equations 3.8, 3.11 , 3.13, 3.15, 3.16) we have calculated EDCS (equation 3.59), TCS (with exchange term, equation 3.53) and, TES (with exchange) in the energy range E = 100 to 700 eV. These results are tabulated in the Tables (3.2), (3.4) . EDCS (equation 3.59) results at incident energies E = 100, 200 and 400 eV are shown in Fig. (3.2) along with the recent theoretical and experimental

data. Considerable exchange correction was observed to the direct DCS (using , equation 3.57), TCS (equation 3.12) and TES (no exchange) . Present results (with the inclusion of second order exchange amplitude (equation 3.58) to that of ESGH process direct amplitude, (equation 3.57) are found in good agreement with the recent experimental data.

Fig. (3.2) shows the present EDCS (equation 3.59) (solid curve C) . This figure shows three sets of results (Set A, Set B and Set C) at incident energies 100, 200 and 400 eV respectively. The notations used for the compared data (theoretical and experimental) are same as given earlier (Fig. 3.2) . It can be observed from the figures (3.1, 3.2) that the present EDCS results (curve C) agree very nicely with the recent measured values (Williams , 1975 ; Van Winger den et al, 1977) than the earlier DCS calculations (curves a' or a), and these exchange corrections to the direct scattering amplitude equation (3.57) are smaller at higher incident energies (Set B, Set C) than at lower incident energy (Set A).

Fig. (3.7) shows the area under the closed curves C' (obtained by EDCS (equation 3.59) X $2\pi \sin\Theta$) and

d' (obtained by DCS (equation 3.2) X $2\pi \sin\theta$) corresponding to the second order (equation 3.58) and first order (equation 3.17) exchange corrections to the direct scattering amplitude (equation 3.57) at incident energy E = 100 eV. It can be noted from this figure that a good amount of exchange correction obtained by the second order exchange term (equation 3.58) than the first order exchange term (equation 3.17) to the TES.

We have displayed our present results in the Tables(3.3 , 3.4 and 3.2). Table (3.3) shows exchange scattering amplitudes (equations 3.56, 3.55 , 3.52) in the incident energy range E = 100, 200, 400 and 600 eV. It can be observed from the Tables(3.3) and (3.1) that the absolute value of exchange real part (equation 3.55) was less than the direct real part (equation 3.13) at $\theta \leq 20^{\circ}$ and greater at $\theta > 20^{\circ}$, but the exchange imaginary contribution (equation 3.52) was always less than that of direct imaginary (equation 3.11) over the entire angular region. Table (3.2) shows the DCS in the incident energy range E = 100 to 700 eV. At each scattering angle θ and incident energy E , two DCS results results are given corresponding to without (lower results) and with (higher results) exchange terms (equations 3.56, 3.55, 3.52) to the direct scattering amplitude (equation

3.57). It can be observed from this table that the present exchange corrections are small, at $\theta \geq 50^{o}$ (fixed energy) and at $E \geq 600$ eV (fixed angle) Table (3.4) shows the TCS (with exchange correction) and TES (with exchange) in the incident energy range E = 100 to 700 eV. These results are found to be in good agreement with the compared theoretical and experimental data.

Finally it was observed from the Tables (3.2, 3.3, 3.4) and Fig. (3.2) that the higher order exchange amplitudes (equations 3.52, 3.55, 3.56) are more important than first order Ochkur exchange amplitude (equation 3.17) to the direct scattering amplitude. And the present results are found to be better than the ESGH (Secs.3.2.1 , 3.2.2) process results.

Table - 3.1

The behaviour of the scattering amplitudes (equations 3.8, 3.13,3.15,3.16,3.17,and 3.9) in ESGH process at the incident E = 100 eV. DCS is expressed in a.u.

θ	$f^{(1)}_{i\to f}$	Rel $f^{(2)}_{HEA}$	Re2 $f^{(2)}_{HEA}$	$f^{(3)}_{GES}$ (-ve)	g_{Och} (-ve)	Im $f^{(2)}_{HEA}$	DCS without exchange	DCS with exchange
	1	2	3	4	5	6	7	8
5	0.979395	0.415584	0.195936	0.023688	0.26455	1.346399	4.09615	4.35525
10	0.922033	0.139775	0.181020	0.063377	0.24398	0.933094	2.21504	2.43999
20	0.744200	0.018177	0.140538	0.117751	0.18222	0.464187	0.83061	0.96622
30	0.559381	0.008547	0.109118	0.128283	0.12208	0.283098	0.38125	0.44954
40	0.413244	0.010811	0.093448	0.117571	0.07860	0.209182	0.20364	0.23612
50	0.309528	0.012109	0.088028	0.105310	0.05082	0.177222	0.12241	0.13814
60	0.238193	0.011881	0.087311	0.093814	0.03375	0.148823	0.08158	0.08961
80	0.154458	0.009936	0.089695	0.076869	0.016671	0.118105	0.04494	0.04752
120	0.088519	0.006808	0.093823	0.059282	0.00641	0.085710	0.02255	0.02312

...Contd.

Table - 3.1 Contd... E = 200 eV

θ	1	2	3	4	5	6	7	8
5	0.959533	0.114182	0.095598	0.020040	0.12867	0.841010	2.00516	2.12862
10	0.854294	0.016395	0.081794	0.045986	0.11004	0.473691	1.04366	1.13767
20	0.586315	0.001812	0.55306	0.064296	0.06527	0.209031	0.37904	0.41731
30	0.378700	0.005168	0.044781	0.056031	0.03451	0.137825	0.15783	0.17089
40	0.251329	0.005899	0.043330	0.048064	0.01837	0.108386	0.07553	0.08015
50	0.175860	0.005299	0.044360	0.040810	0.01034	0.089799	0.04213	0.04395
60	0.129755	0.004476	0.045640	0.035458	0.00622	0.076065	0.02644	0.02725
80	0.080631	0.003172	0.047440	0.028349	0.00272	0.057389	0.01339	0.01361
120	0.045014	0.001932	0.048918	0.021217	0.00094	0.039150	0.00623	0.00627

.... Contd..

Table - 3.1 Contd... E = 400 eV

θ	1	2	3	4	5	6	7	8
5	0.921850	0.016124	0.045148	0.015863	0.455267	0.06098	1.14114	1.19728
10	0.742703	0.001124	0.034176	0.029494	0.220381	0.04543	0.60546	0.63920
20	0.405366	0.002163	0.022461	0.029118	0.101754	0.01909	0.17104	0.17878
30	0.224970	0.002869	0.021673	0.022850	0.072322	0.00771	0.05661	0.05835
40	0.1374928	0.002324	0.022697	0.018236	0.055735	0.00345	0.02401	0.02449
50	0.092727	0.001771	0.023527	0.015151	0.044280	0.00174	0.01244	0.01260
60	0.067011	0.001366	0.024059	0.012959	0.036144	0.00097	0.00747	0.00754
80	0.040899	0.000888	0.024616	0.010092	0.025937	0.00039	0.00361	0.00362
120	0.022621	0.000512	0.024995	0.007301	0.016907	0.00013	0.00162	0.00162

Table - 3.2

DCS for ESGH process (Sec. 3.2.1 and Sec. 3.5.1) at the incident energies 100 to 700 eV , with (equ. 3.59) and without (equ. 3.57) exchange terms (3.52, 3.55, 3.56). DCS expressed in a.u.

E	θ = 5°	10°	20°	30°	40°	50°	60°
	4.09615	2.21504	0.83061	0.38125	0.20364	0.12241	0.08158
100							
	4.85478	2.70244	1.07472	0.49983	0.26143	0.15267	0.09943
	2.00516	1.04366	0.37904	0.15783	0.07553	0.04213	0.02644
200							
	2.21816	1.18453	0.43471	0.17761	0.08337	0.04601	0.02889
	1.39889	0.74831	0.24223	0.08845	0.03941	0.02097	0.01278
300							
	1.51089	0.81977	0.26369	0.09464	0.04171	0.02218	0.01363
	1.14114	0.60546	0.17104	0.05661	0.02401	0.01244	0.00747
400							
	1.21499	0.64897	0.18131	0.05919	0.02496	0.01299	0.00789

....Contd..

Table - 3.2 Contd...

E	θ = 5°	10°	20°	30°	40°	50°	60°
500	1.00094	0.51330	0.12713	0.03918	0.01608	0.00821	0.00488
	1.05498	0.54233	0.13272	0.04047	0.01657	0.00851	0.00514
600	0.91077	0.44541	0.09803	0.02863	0.01149	0.00580	0.00343
	0.95269	0.46591	0.10134	0.02936	0.01178	0.00600	0.00361
700	0.84567	0.39196	0.07778	0.02179	0.00861	0.00432	0.00255
	0.87943	0.40702	0.07988	0.02224	0.00879	0.00446	0.00267

For each incident energy E there are two results upper one is without exchange correction and lower one is with higher order exchange terms.

Table - 3.3

Behaviour of the exchange amplitudes (equs. 3.56, 3.55, 3.52) from E = 100 to 600 eV.

E	θ	$\bar{g}_{B1}$	Re $g^{(2)}_{HEA}$	Im $g^{(2)}_{HEA}$
	5	-0.23709	-0.12999	0.09967
	10	-0.21653	-0.12235	0.08732
	20	-0.15477	-0.09964	0.05274
	30	-0.09463	-0.07819	0.02374
	40	-0.05114	-0.06378	0.00713
100	50	-0.02336	-0.05567	-0.00048
	60	-0.00630	-0.05158	-0.00335
	80	0.01078	-0.04893	-0.00399
	120	0.02105	-0.04903	-0.00235
	5	-0.12457	-0.04518	0.04242
	10	-0.10591	-0.03957	0.03322
	20	-0.06114	-0.026263	0.01350
	30	-0.03037	-0.01760	0.00299
	40	-0.01424	-0.01361	-0.00060
200	50	-0.00621	-0.01204	-0.00142
	60	-0.00209	-0.01151	-0.00138
	80	0.00142	-0.01141	-0.00091
	120	0.003190	-0.01169	-0.00036

....Contd.

Table - 3.3 Contd...

E	θ	$\bar{g}_{B1}$	Re $g^{(2)}_{HEA}$	Im $g^{(2)}_{HEA}$
	5	-0.06041	-0.01576	0.01698
	10	-0.04486	-0.01212	0.01086
	20	-0.01853	-0.00608	0.00218
	30	-0.00714	-0.00370	-0.00023
	40	-0.00288	-0.00299	-0.00057
400	50	-0.00177	-0.00280	-0.00049
	60	-0.00041	-0.00277	-0.00036
	80	0.00018	-0.00282	-0.00019
	120	00.00044	-0.00289	-0.00066
	5	-0.03841	-0.00834	0.00958
	10	-0.02526	-0.00573	0.00511
	20	-0.00817	-0.00242	0.00049
	30	-0.002723	-0.00149	-0.00029
	40	-0.00102	-0.00128	-0.00024
600	50	-0.00040	-0.00124	-0.00021
	60	-0.00014	-0.00124	-0.00015
	80	0.00005	-0.00126	-0.00007
	120	0.00014	-0.00129	-0.00003

Table - 3.4

TCS and TES corresponding to the equations (3.12, 3.53, 3.24 and 3.59) respectively for the incident energies 100 to 700 eV for the ESGH and the ESEH processes.

E eV	ESGH							ESEH	
	TCS	ETCS	ETCS + TCS	UEBS	Expt	TES	UEBSI	TCS	ESEH,TCS / ESGH,TCS
100	7.5615	0.4837	8.0452	7.19	1.83	2.03	1.43	150.231	19.868
200	4.3685	0.1510	4.5195	4.27	0.789	0.772	0.613	83.402	19.092
300	3.1423	0.0756	3.2179	3.10	-	0.453	0.382	58.834	18.725
400	2.4793	0.0461	2.5254	2.45	-	0.323	0.276	45.846	18.492
500	2.0595	0.0313	2.0908	-	-	0.244	-	37.745	18.328
600	1.7681	0.0228	1.7909	-	-	-	-	32.181	18.201
700	1.5531	0.0174	1.5705	-	-	-	-	28.111	18.099

UEBS = Results taken from Byron et al (1982)
UEBSI = Results taken from Byron et al (1982)
Expt = Experimental results (Total Elastic Cross Section) taken from Van Wingerden et al (1977).

Table - 3.5

Behaviour of the Born scattering amplitudes (equations 3.38, 3.39, 3.40) in ISH process at E = 100 eV.

θ	$\mathrm{Re1}\ f^{(2)}_{HEA}$ (-ve)	$\mathrm{Re1}'\ f^{(2)}_{HEA}$ (-ve)	$\mathrm{Re2}\ f^{(2)}_{HEA}$ (-ve)	$\mathrm{Re2}'\ f^{(2)}_{HEA}$ (-ve)	$f^{(3)}_{GES}$	$\mathrm{Im}\ f^{(2)}_{HEA}$ (-ve)	$\mathrm{Im}\ f'^{(2)}_{HEA}$ (-ve)
	1	2	3	4	5	6	7
0	0.48896	0.35679	0.69118 -1	0.70445 -1	0.15522 -2	0.10238 +1	0.11604 +1
5	0.21137	0.11323	0.60649 -1	0.61051 -1	0.34289 -2	0.73067	0.75375
10	0.49272 -1	0.14817 -1	0.42008 -1	0.40708 -1	0.45930 -2	0.37374	0.36112
20	0.20092 -1	0.11491 -1	0.17907 -1	0.16148 -1	0.45729 -3	0.13587	0.13453
30	0.24563 -1	0.16715 -1	0.21785 -1	0.21838 -1	0.32089 -2	0.10847	0.11095
40	0.19890 -1	0.13600 -1	0.30680 -1	0.31652 -1	0.31165 -2	0.92109 -1	0.94175 -1
50	0.14308 -1	0.97317 -2	0.35872 -1	0.37022 -1	0.26967 -2	0.73514 -1	0.74859 -1
60	0.10281 -1	0.69622 -2	0.38027 -1	0.39139 -1	0.21596 -2	0.57677 -1	0.58557 -1
80	0.59273 -2	0.39957 -2	0.38772 -1	0.39752 -1	0.13839 -2	0.37149 -1	0.37599 -1
120	0.30307 -2	0.20381 -2	0.38090 -1	0.38985 -1	0.72195 -3	0.20618 -1	0.20831 -1

...Contd..

Table - 3.5 Contd...

E= 400 eV

θ	1	2	3	4	5	6	7
0	0.28315	0.20618	0.18506 -1	0.18603 -1	0.13059 -3	0.76931	0.84252
5	0.14523 -2	0.24209 -2	0.10095 -1	0.98108 -2	0.11504 -2	0.17903	0.17291
10	0.40851 -2	0.24659 -2	0.37476 -2	0.34687 -2	0.75083 -4	0.65964 -1	0.65497 -1
20	0.49312 -2	0.33209 -2	0.82815 -2	0.83749 -2	0.77187 -3	0.46063 -1	0.46339 -1
30	0.23389 -2	0.15673 -2	0.99728 -2	0.10059 -1	0.49544 -3	0.26926 -1	0.27028 -1
40	0.12486 -2	0.83497 -3	0.99895 -2	0.10056 -1	0.29255 -3	0.16118 -1	0.16164 -1
50	0.77394 -3	0.51721 -3	0.98304 -2	0.98899 -2	0.18228 -3	0.10543 -1	0.10570 -1
60	0.53389 -3	0.35669 -3	0.97072 -2	0.97642 -2	0.12082 -3	0.74624 -2	0.74809 -2
80	0.31145 -3	0.20805 -3	0.95719 -2	0.96276 -2	0.62300 -4	0.44410 -2	0.44517 -2
120	0.16736 -3	0.11179 -3	0.94799 -2	0.95354 -2	0.26736 -4	0.24073 -2	0.24130 -2

' (Prime) Results corresponding to DE = 0.250

Without prime results corresponding to DE = 0.375

Table - 3.6

DCS for ISH process (Sec. 3.4.1) at incident energies 100 to 700 eV , with DE = 0.250 and DE = 0.375 in equations (3.37, 3.38, 3.39).

E	Θ = 0°	5°	10°	20°	30°	40°	50°
100	0.24090 +1	0.14205 +1	0.69337	0.16230	0.41742 -1	0.16431 -1	0.81678 -2
	0.22298 +1	0.14176 +1	0.70607	0.16415	0.41518 -1	0.16143 -1	0.80183 -2
200	0.20681 +1	0.90228	0.35688	0.40378 -1	0.77688 -2	0.26265 -2	0.11251 -2
	0.19440 +1	0.91372	0.35948	0.40362 -1	0.76999 -2	0.26040 -2	0.11172 -2
300	0.18690 +1	0.70668	0.21666	0.14572 -1	0.24961 -2	0.78418 -3	0.32032 -3
	0.17728 +1	0.71201	0.21742	0.14526 -1	0.24811 -2	0.78041 -3	0.31903 -3
400	0.17401 +1	0.59085	0.13922	0.64888 -2	0.10585 -2	0.32145 -3	0.12923 -3
	0.16606 +1	0.59339	0.13949	0.64659 -2	0.10541 -2	0.32042 -3	0.12888 -3

....Contd..

Table - 3.6 Contd...

E	θ = 0°	5°	10°	20°	30°	40°	50°
500	0.16489 +1	0.50649	0.92654 -1	0.33320 -2	0.53283 -3	0.15929 -3	0.63743 -4
	0.15808 +1	0.50784	0.92761 -1	0.33214 -2	0.53123 -3	0.15891 -3	0.63609 -4
600	0.15806 +1	0.43951	0.63511 -1	0.18951 -2	0.30129 -3	0.89457 -4	0.35794 -4
	0.15207 +1	0.44030	0.63552 -1	0.18897 -2	0.30061 -3	0.89291 -4	0.35733 -4
700	0.15270 +1	0.38419	0.44664 -1	0.11638 -2	0.18526 -3	0.54878 -4	0.21997 -4
	0.14734 +1	0.38469	0.44677 -1	0.11609 -2	0.18492 -3	0.54795 -4	0.21966 -4

For each incident energy there are two results upper one i corresponds to DE = 0.250 and lower one corresponds to DE = 0.375.

Table - 3.7

The comparison of present DCS with the other theoretical results at E = 100 and 200 eV.

	E = 100 eV			E = 200 eV		
θ	Ref(1)	Ref(2)	Present	Ref(1)	Ref(2)	Present
0	9.3 -1	3.57	2.22970	1.20	3.33	1.944
10	3.0 -1	3.65 -1	0.70607	2.5 -1	2.6 -1	0.3595
20	6.8 -2	8.8 -2	0.16416	2.3 -2	2.8 -2	0.4036 -1
30	1.10 -2	2.0 -2	0.41518 -1	2.8 -3	4.2 -3	0.76998 -2
40	3.4 -3	7.6 -3	0.16143 -1	1.16 -3	1.56 -3	0.2604 -2
60	1.6 -3	2.7 -3	0.4423 -2	2.9 -4	4.1 -4	0.5549 -3
80	7.6 -4	1.28 -3	0.1665 -2	1.35 -4	1.61 -4	0.1897 -3
100	4.2 -4	7.1 -4	0.80309 -3	5.6 -5	8.0 -5	0.8926 -4
120	2.8 -4	4.7 -4	0.47667 -3	4.1 -5	5.1 -5	0.52796 -4

Ref(1) Bransden et al (1982)

Ref(2) Kingston et al (1976).

Table 3.8

The Behaviour of Born scattering amplitudes (equations 3.26, 3.27, 3.28, 3.29, 3.24) in ESEH process at incident energy E = 200 eV and 400 eV.

E = 200 eV

θ	Re1 $f^{(2)}_{HEA}$	Re2 $f^{(2)}_{HEA}$	$F^{(3)}_{GES}$ (-ve)	g_{Och} (- ve)	Im $f^{(2)}_{HEA}$	DCS (no exchange)	DCS (With exchange)
	1	2	3	4	5	6	7
10	0.32407 -1	0.14482	0.23467 -2	0.18210 -2	0.16008 +1	23.36025	23.36830
20	0.23153 -1	0.19799	0.39612 -3	0.45300 -2	0.90670	2.44295	2.44789
30	0.10903 -1	0.20068	0.38212 -4	0.46181 -2	0.51321	0.70069	0.70296
40	0.63310 -2	0.20053	0.19859 -4	0.26452 -2	0.33331	0.30662	0.30738
50	0.41883 -2	0.20086	0.27310 -4	0.14756 -2	0.23855	0.16800	0.16828
60	0.30121 -2	0.20121	0.24472 -4	0.87006 -3	0.18219	0.10583	0.10595
80	0.18356 -2	0.20166	0.16483 -4	0.36791 -3	0.12100	0.54474 -1	0.54504 -1
120	0.10165 -2	0.20201	0.84980 -5	0.12342 -3	0.73728	0.25787 -1	0.25792--1

Contd...

Table 3.8 Contd....

E = 400 eV

θ	1	2	3	4	5	6	7
10	0.18093 -1	0.88016 -1	0.62024 -3	0.44189 -2	0.91507	6.30973	6.31541
20	0.60463 -2	0.10043	0.30158 -4	0.24686 -2	0.39305	0.55880	0.56014
30	0.27763 -2	0.10035	0.12171 -4	0.11100 -2	0.21187	0.15729	0.15757
40	0.16093 -2	0.10062	0.12667 -4	0.48453 -3	0.13592	0.68323 -1	0.68393 -1
50	0.10609 -2	0.10082	0.94260 -5	0.23769 -3	0.96421	0.37415 -1	0.37437 - 1
60	0.76081 -3	0.10095	0.67847 -5	0.13055 -3	0.73109 -1	0.23651 -1	0.23660 -1
80	0.46205 -3	0.10107	0.37652 -5	0.51411 -4	0.48057 -1	0.12310 -1	0.12312 -1
120	0.25519 -3	0.10116	0.16937 -5	0.16412 -4	0.28969 -1	0.59376 -1	0.59379 -2

Table - 3.9

DCS for ESEH process (Sec. 3.3.1) for incident energies 100 to 700 eV, with and without Re $f^{(2)}_{HEA}$ (equation 3.27) in DCS (no exchange).

E	θ = 5°	10°	20°	30°	40°	50°	60°
100	0.19026 +3	0.61452 +2	0.85468 +1	0.23943 +1	0.96113	0.47624	0.27172
	0.20348 +3	0.65978 +2	0.10129 +2	0.31701 +1	0.14094 +1	0.77288	0.48563
200	0.10715 +3	0.22131 +2	0.20143 +1	0.50453	0.19253	0.92456 -1	0.51500 -1
	0.11123 +3	0.23360 +2	0.24429 +1	0.70069	0.30662	0.16800	0.10583
300	0.74404 +2	0.10552 +2	0.83741	0.20345	0.75836 -1	0.35752 -1	0.19633 -1
	0.76323 +2	0.11179 +2	0.10293 +1	0.29154	0.12706	0.69583 -1	0.43909 -1
400	0.54569 +2	0.59262 +1	0.45043	0.10735	0.39343 -1	0.18314 -1	0.99620 -2
	0.55565 +2	0.63097 +1	0.55879	0.15729	0.68323 -1	0.37414 -1	0.23651 -1

...Contd..

Table - 3.9 Contd...

E	Θ= 5°	10°	20°	30°	40°	50°	60°
500	0.41246 +2	0.37207 +1	0.27947	0.65564 -1	0.23719 -1	0.10939 -1	0.59094 -2
	0.41875 +2	0.39773 +1	0.34914	0.97698 -1	0.42330 -1	0.23189 -1	0.14682 -1
600	0.31888 +2	0.25297 +1	0.18964	0.43893 -1	0.15721 -1	0.71994 -2	0.38685 -2
	0.32329 +2	0.27119 +1	0.23825	0.66296 -1	0.28674 -1	0.15717 -1	0.99663 -2
700	0.25124 +2	0.18245 +1	0.13681	0.31302 -1	0.11123 -1	0.50646 -2	0.27099 -2
	0.25458 +2	0.19598 +1	0.17267	0.47808 -1	0.20653 -1	0.11329 -1	0.71925 -2

For each incident energy there are two results upper one is without Re2 $f^{(2)}_{HEA}$ in DCS ,lower one is with Re2 $f^{(2)}_{HEA}$ in DCS .

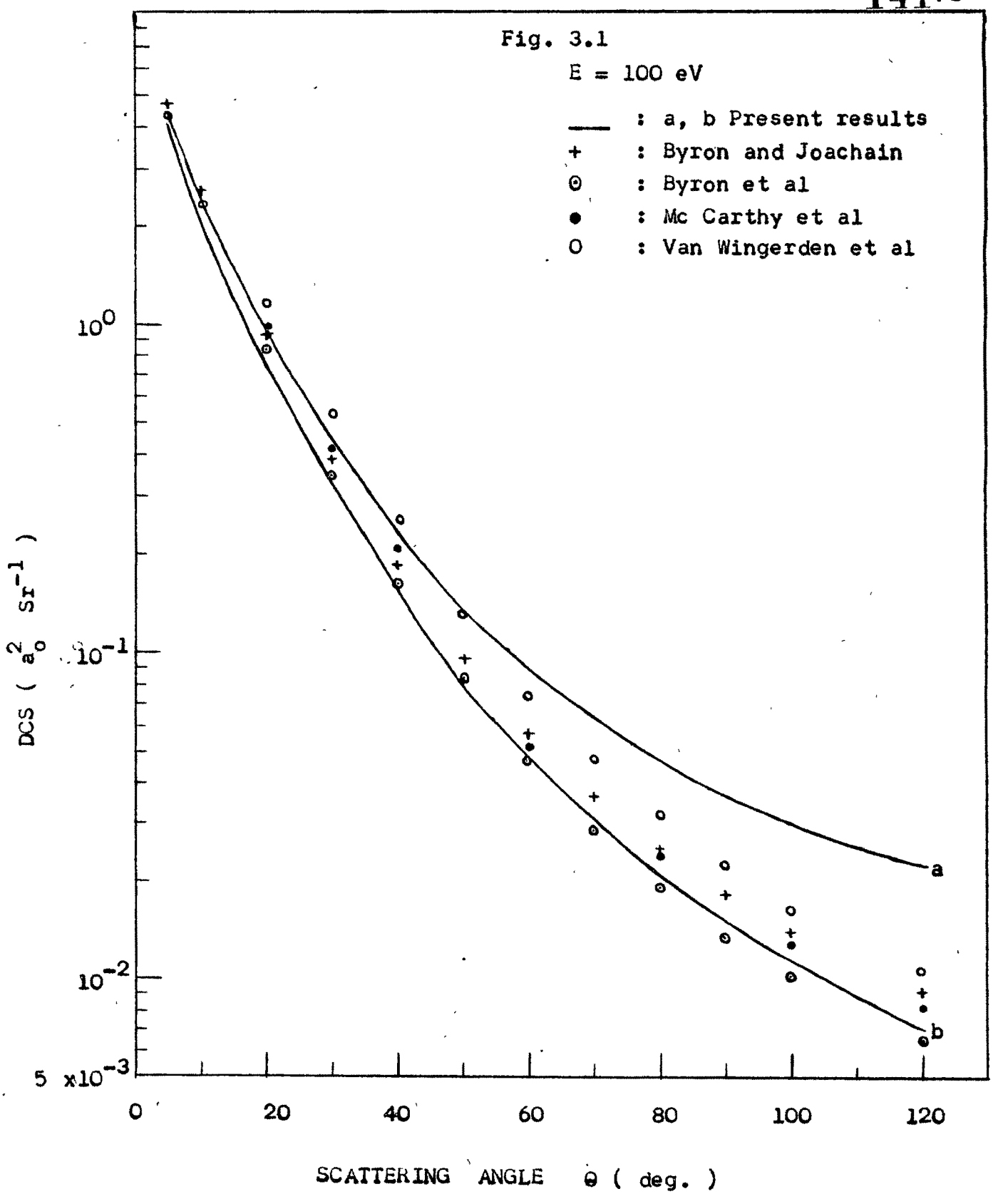
Fig. 3.1
E = 100 eV
: a, b Present results
: Byron and Joachain
: Byron et al
: Mc Carthy et al
: Van Wingerden et al
10^0
10^{-1}
10^{-2}
5×10^{-3}
DCS (a_o^2 sr^{-1})
0
20
40
60
80
100
120
SCATTERING ANGLE θ (deg.)
a
b

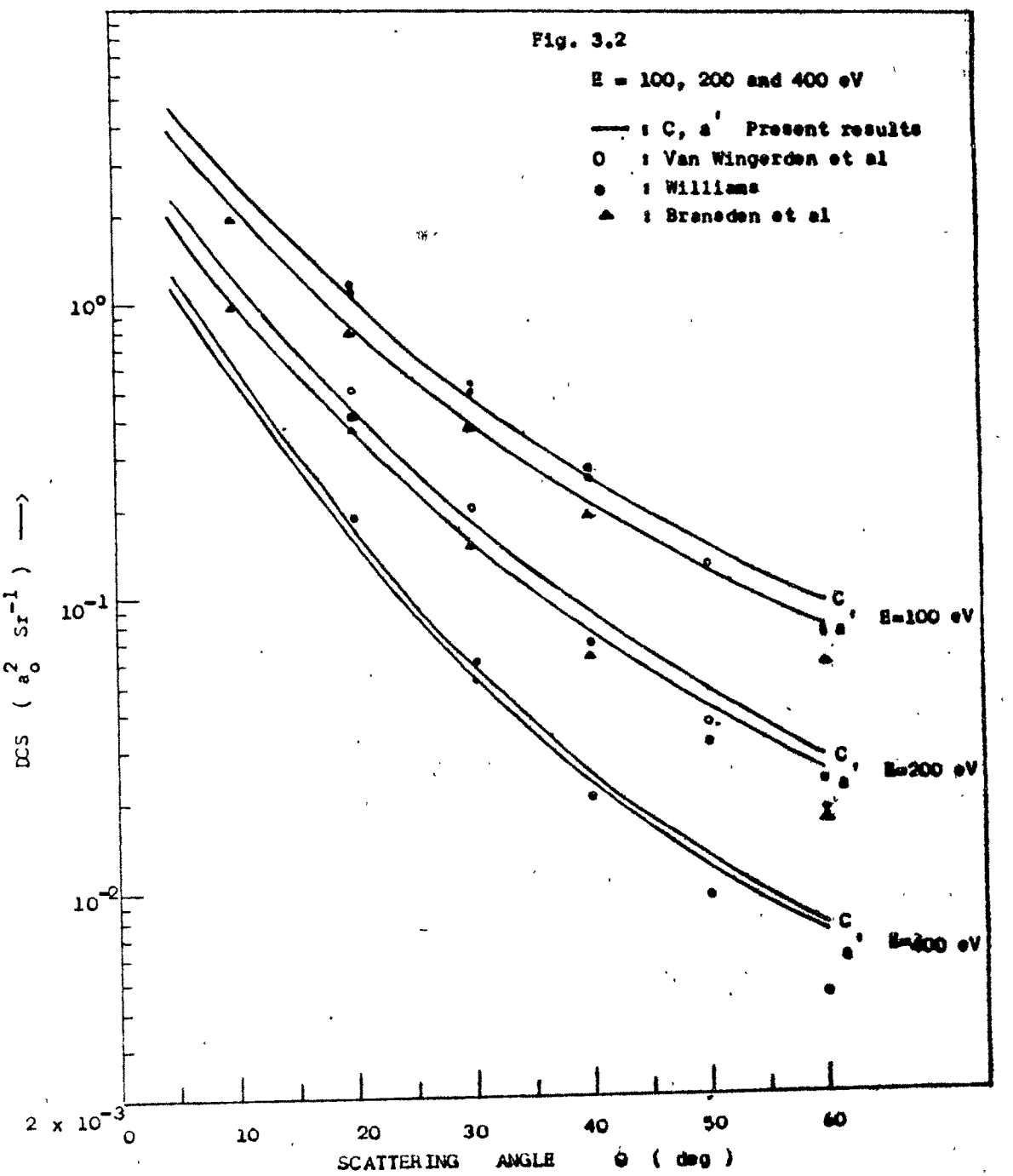
Fig. 3.2
E = 100, 200 and 400 eV
—— : C, a' Present results
O : Van Wingerden et al
● : Williams
▲ : Braneden et al
C, a' E=100 eV
C, a' E=200 eV
C, a' E=400 eV
DCS (a_o^2 sr^{-1}) ⟶
10^0
10^{-1}
10^{-2}
2×10^{-3}
0
10
20
30
40
50
60
SCATTERING ANGLE θ (deg)

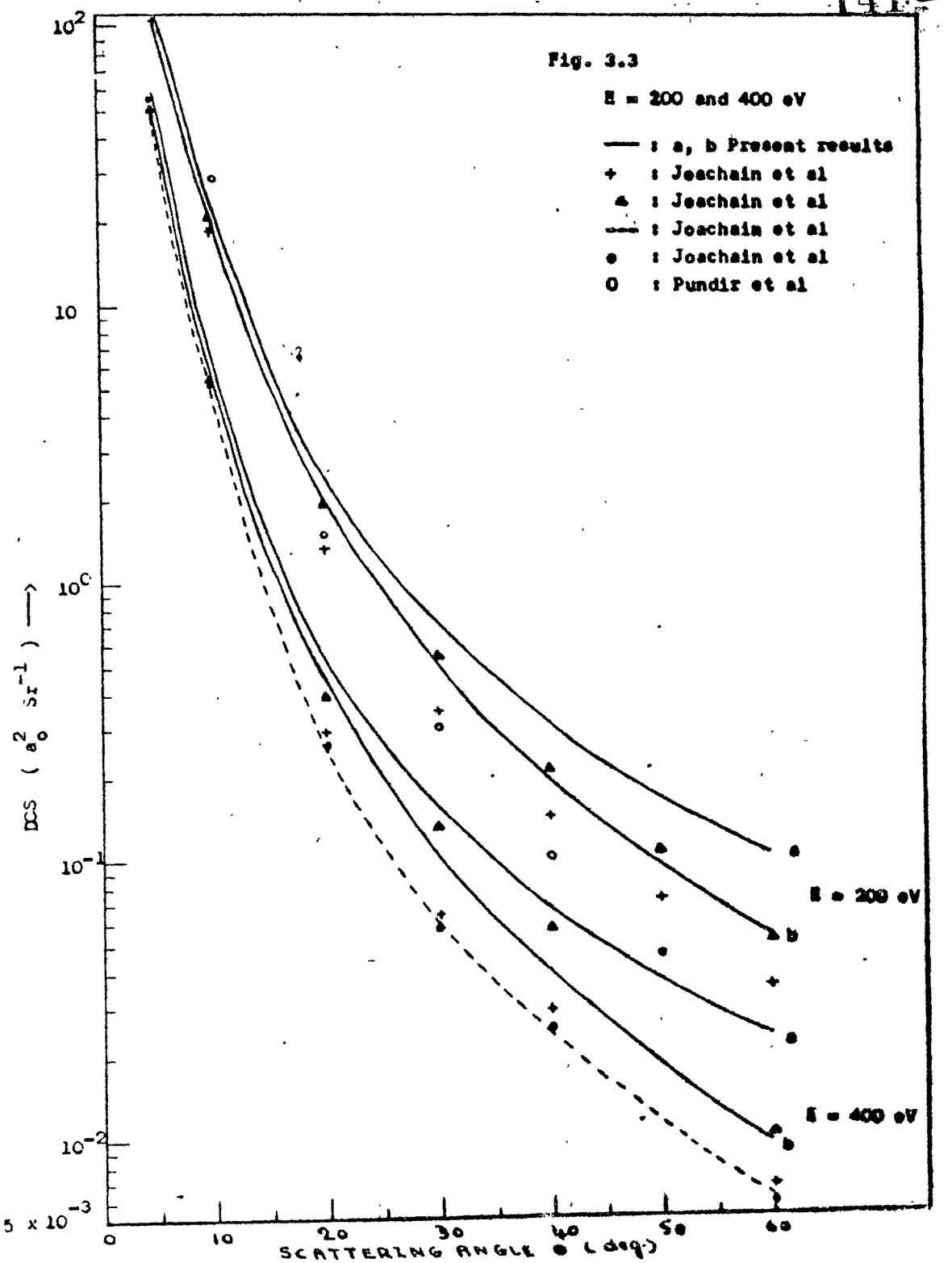
Fig. 3.3
E = 200 and 400 eV
—— : a, b Present results
+ : Joachain et al
▲ : Joachain et al
—— : Joachain et al
● : Joachain et al
O : Pundir et al
E = 200 eV
E = 400 eV
a
b
DCS (a_0^2 sr^{-1}) ⟶
SCATTERING ANGLE θ (deg)
10^2
10
10^0
10^{-1}
10^{-2}
5×10^{-3}
0
10
20
30
40
50
60

Fig. 3.4B

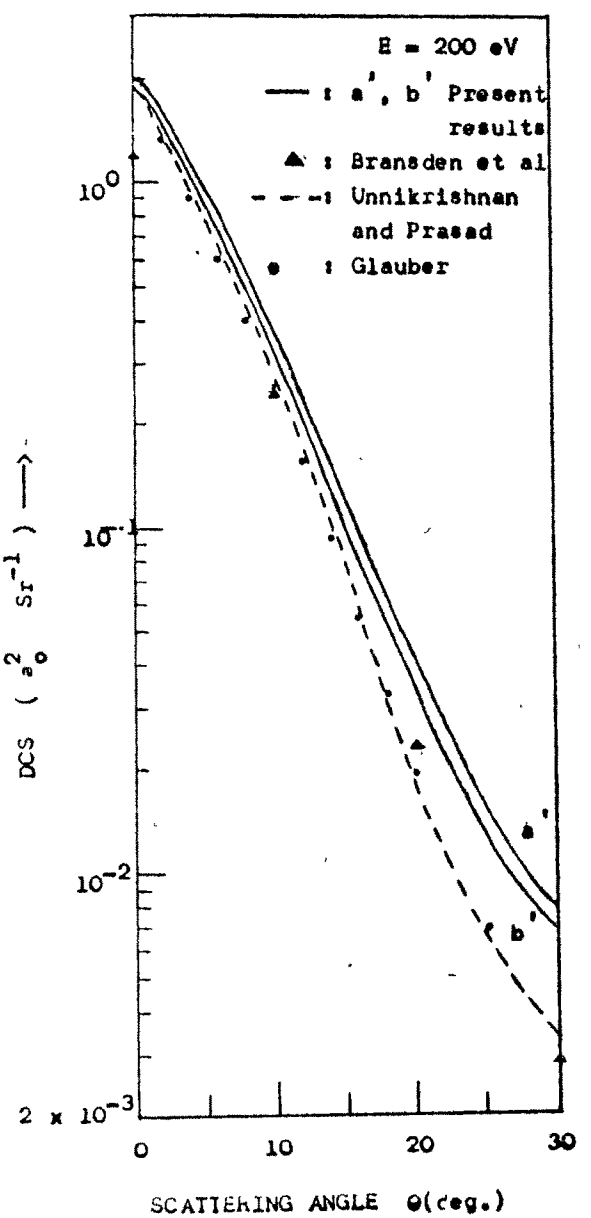

Fig. 3.4A

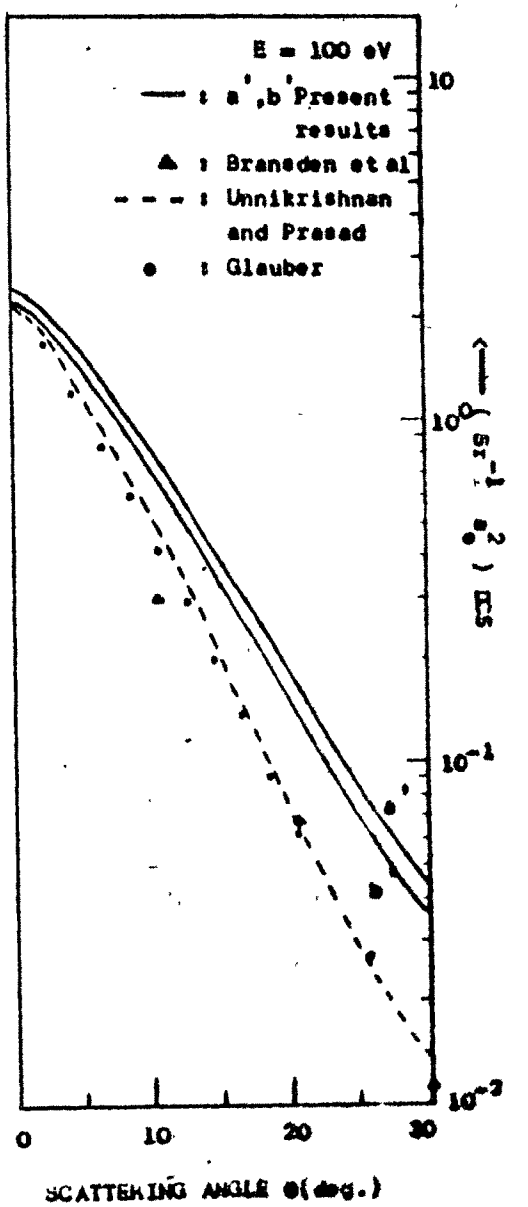

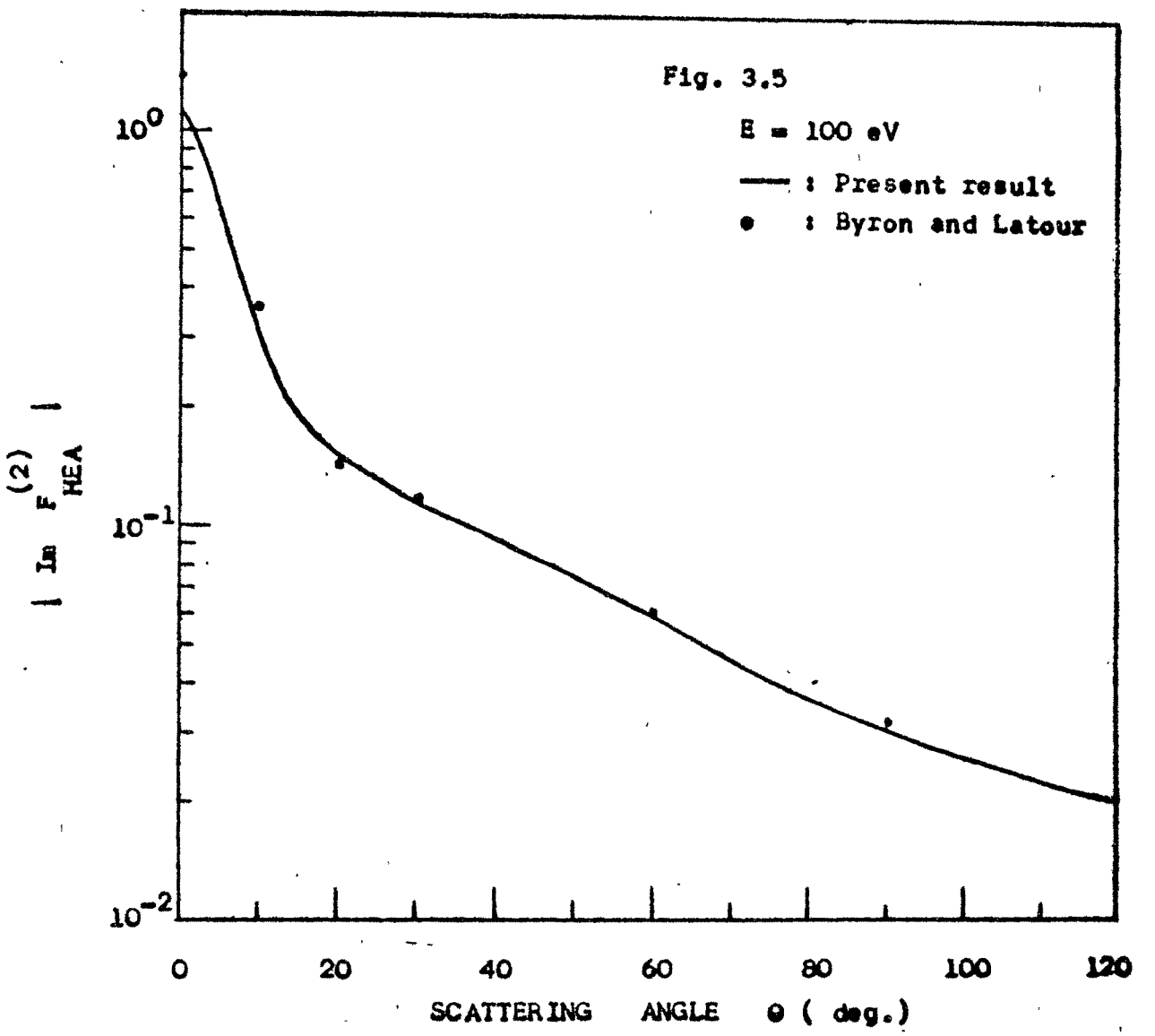
Fig. 3.5
E = 100 eV
: Present result
: Byron and Latour
10^0
10^{-1}
10^{-2}
$|\ \mathrm{Im}\ F^{(2)}_{HEA}\ |$
0
20
40
60
80
100
120
SCATTERING ANGLE θ (deg.)

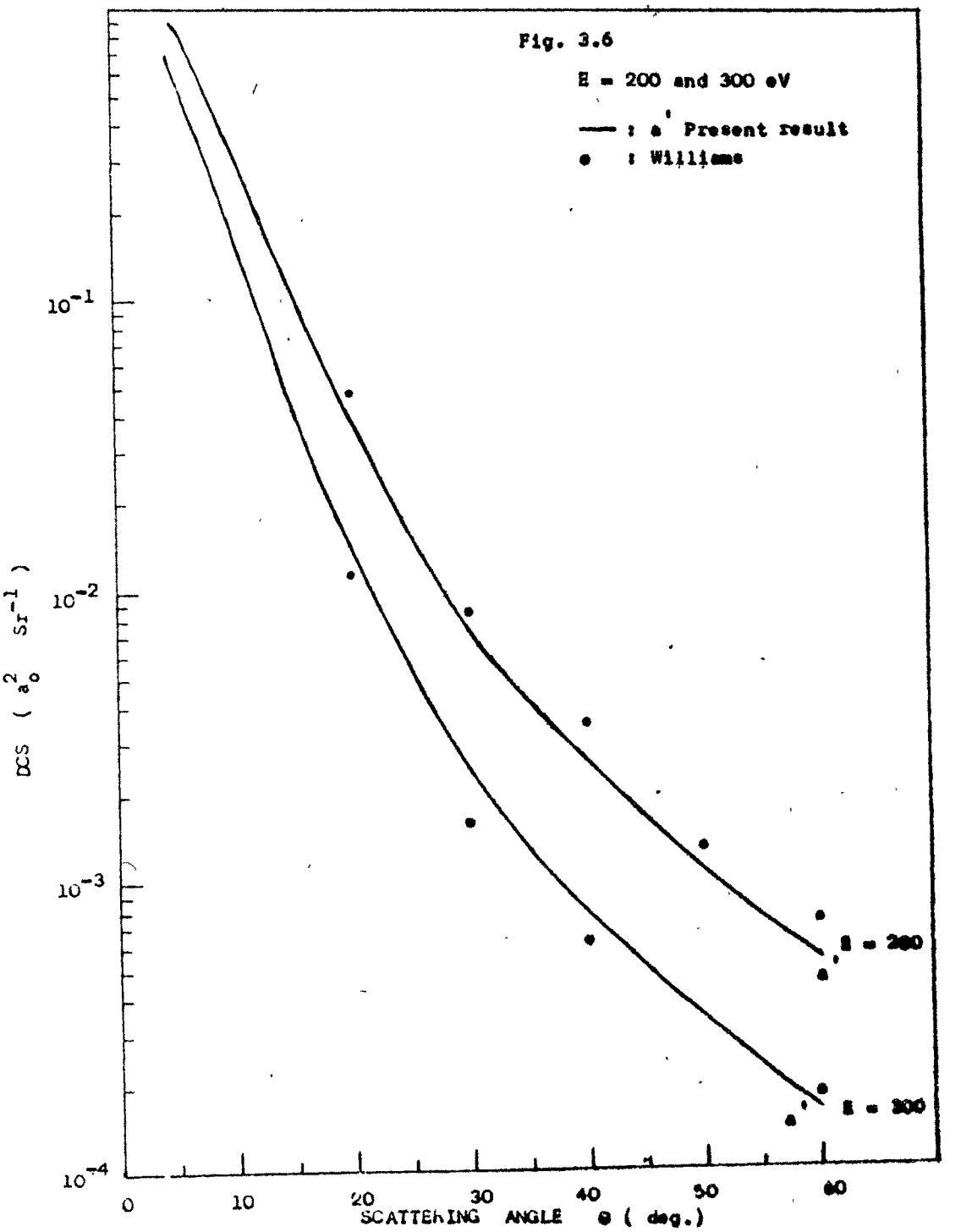
Fig. 3.6
E = 200 and 300 eV
—— : a' Present result
• : Williams
E = 200
E = 300
DCS (a_o^2 sr^{-1})
10^{-1}
10^{-2}
10^{-3}
10^{-4}
0
10
20
30
40
50
60
SCATTERING ANGLE θ (deg.)

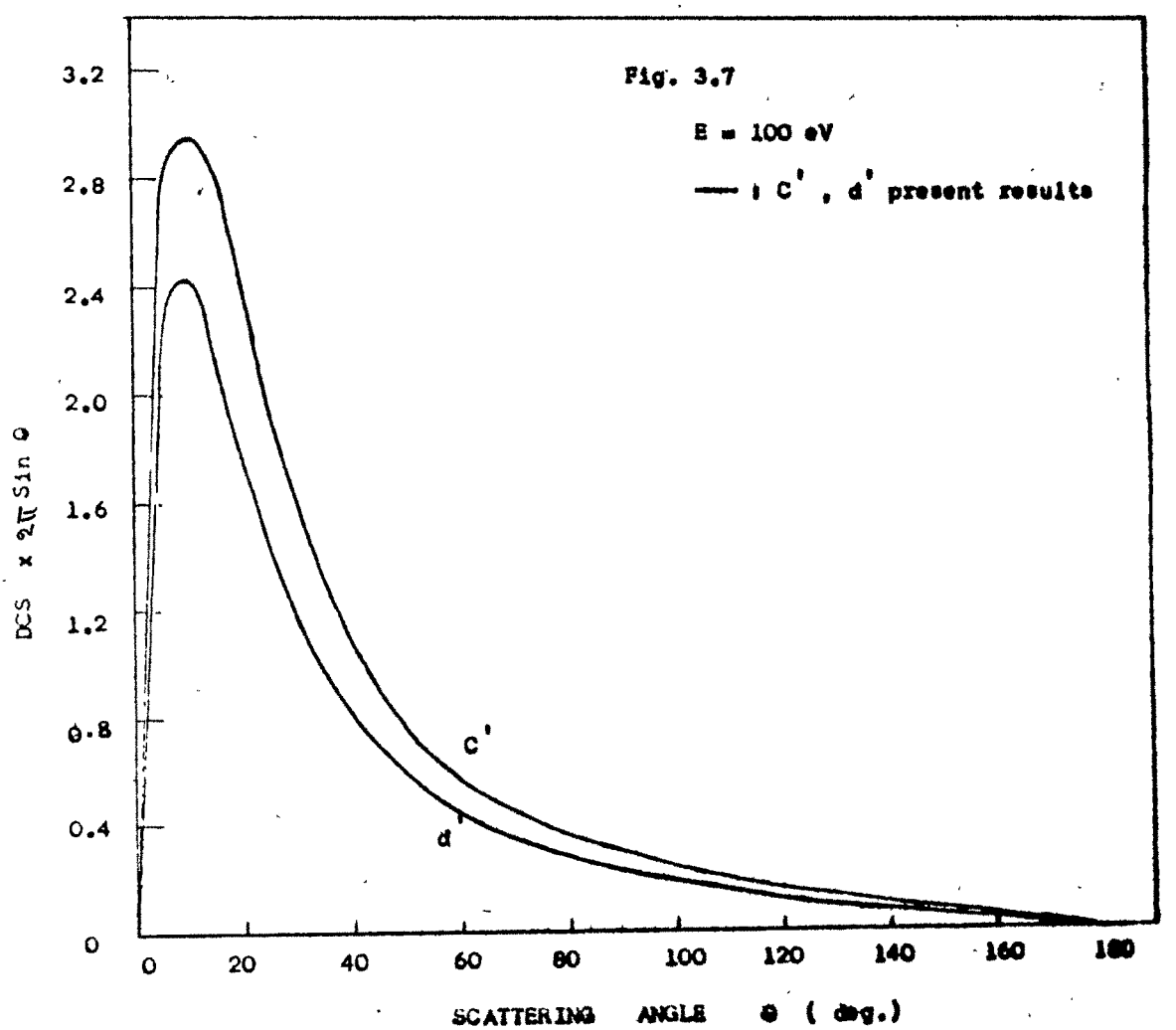
Fig. 3.7
E = 100 eV
—— : C' , d' present results
C'
d'
DCS x 2π Sin θ
3.2
2.8
2.4
2.0
1.6
1.2
0.8
0.4
0
0
20
40
60
80
100
120
140
160
180
SCATTERING ANGLE θ (deg.)